Journal of the Atmospheric Sciences

Observations of the Development and Vertical Structure of the Lake Breeze Circulation During the 2017 Lake Michigan Ozone Study

--Manuscript Draft--

Manuscript Number:	JAS-D-20-0297
Full Title:	Observations of the Development and Vertical Structure of the Lake Breeze Circulation During the 2017 Lake Michigan Ozone Study
Article Type:	Article
Abstract:	Ground-based thermodynamic and kinematic profilers were placed adjacent to the western shore of Lake Michigan at two sites as part of the 2017 Lake Michigan Ozone Study. The southern site near Zion, Illinois, hosted a microwave radiometer (MWR) and a sodar wind profiler, while the northern site in Sheboygan, Wisconsin, featured an Atmospheric Emitted Radiance Interferometer (AERI), a Doppler lidar, and a High Spectral Resolution Lidar (HSRL). Each site experienced several lake breeze events during the experiment. Composite time series and time/height cross sections were constructed relative to the lake breeze arrival time so that commonalities across events could be explored. The composited surface observations indicate that the initial post-breeze wind direction is consistently southeasterly at both sites regardless of pre-breeze wind direction. Surface relative humidity increases with the arriving lake breeze, though this is due to cooler air temperatures as absolute moisture content stays the same or decreases. The profiler observations show that the vertical structure of the lake breeze depends greatly on the local degree of thermodynamic instability: when unstable lapse rates are found in the lower troposphere, the lake breeze grows deeper and penetrates further inland than with stable lapse rates. The cold air associated with the lake breeze remains confined to the lowest 200 m of the troposphere even if the wind shift is observed at higher altitudes. The evolution of the lake breeze corresponds well to observed changes in baroclinicity and calculated changes in circulation. Collocated observations of aerosols and particulate matter show increases during the lake breeze as well.

Once again, we thank the editor and reviewers as we iterate towards a manuscript that is appropriate for publication in JAS. Your contributions have been invaluable and we are grateful for the effort that you have put into improving our own work.

Reviewer #1

General Comments
==========

The authors have substantially improved the paper. There are a number of minor comments listed below.

Thank you for your kind words regarding our work. We appreciate that your comments have been in the spirit of improving this manuscript and making it scientifically robust and useful to the community.

The following reviewer comment addressing the number of cases is detailed, and we are reprinting it in its entirety ahead of addressing it. We apologize in advance, for we have taken 1500 words to say that we stand behind our analysis in its original form. Hopefully, however, it will help you understand our motivation and reasoning behind our approach.

But first and more importantly...it still seemed unlikely to me that there were only 6 lake breeze events over the course of May 22 to Jun 22 on the western shore of Lake Michigan. I thought I'd have a closer look. There is a good website for archived weather maps and so on at https://www2.mmm.ucar.edu/imagearchive/. I found a regional surface station map centered on MSP available at hourly intervals. I examined the surface station maps, looking for evidence of lake-breeze circulations on Lake Michigan. I looked for maps showing mostly clear conditions in the area in the afternoon, wind shifts to onshore, onshore winds at multiple shoreline locations around the perimeter of the lake, and the resulting wind divergence pattern over the Lake. I went through without looking at which six events were identified in the study.

Just using this one resource, I found clear evidence of the Lake Michigan lake breeze affecting the study area on the following days:

- May 25, 26, 27, 28
- June 1, 2, 6, 7, 8, 9, 11, 13, 15, 16, 17

Only 5 of those overlap with the events identified in the study. Note that a well-developed lake-breeze front may not be present for all of these days.

There were numerous other instances of a Lake Michigan lake-breeze circulation, but for these the lake breeze penetrated inland only in areas to the north and/or south of the study area.

On June 12th, however, a synoptic-scale boundary was drifting south through WI and MN. Winds across multiple states were S-SW south of this boundary and NE-NW to the north of this boundary. Unfortunately, it appears this synoptic-scale boundary was identified as a lake-breeze front in the study, despite the claim in the paper that "Analysis of contemporaneous surface maps helps illustrate this last point: in all cases, any synoptic scale disturbances were either hundreds of km removed from the observing sites, were stationary, or did not propagate over the observation domain until after the period analyzed in this paper." The wind shift, change in temperature, etc. would certainly have been quite similar to that of a lake-breeze front passage.

So, a couple things. One - the lake breeze composites all contain a non-lake breeze event and obviously that needs to be corrected.

Two - the reason for the limited set of lake breezes days must be explained. For the 5 lake breeze events identified, is there something that differentiates them from the other lake breeze events I have identified above (e.g. strong lake-breeze front)? If not, and there is no good explanation for using just these 5 events, then the authors should review all potential cases again, with particular emphasis on days I have identified, and ensure all days with a lake-breeze front in the study area are actually included. The larger sample size would also improve the composites and the applicability of the results.

In the paper, we took care to outline the criteria by which we identified the passage of lake breeze fronts at our observation sites. As a reminder, they are as follows:

1. The zonal (u) component of the surface wind reversed from offshore to onshore.
2. Surface temperatures dropped abruptly with the wind shift.
3. Mixing height decreased with the wind shift.
4. No rain was detected within three hours of the wind shift.

These criteria were evaluated using instrumentation at the two supersites. 1 and 2 were assessed using the surface meteorological instrumentation, and 3 was calculated from the thermodynamic profiles retrieved by the AERI or MWR. For Zion, 4 was determined by the MWR's on-board rain sensor while at Sheboygan it was determined by noting when the AERI's automated precipitation-sensing hatch door was closed.

The reviewer goes above and beyond the call of duty by identifying potential cases for our work. However, we had already considered these days. Here is a table identifying the reasons for our decisions on those particular days using the instrumentation at Zion:

May	
25	mixed layer does not develop
26	mixed layer does not develop; onshore flow is consistent with synoptic pattern
27	mixed layer does not develop; no clear decrease in surface temperature
28	mixed layer does not develop

June	
1	mixed layer does not develop
2	**Included Case**
6	mixed layer does not develop; no clear change from offshore to onshore flow; onshore flow is consistent with synoptic pattern
7	mixed layer does not develop; no clear change from offshore to onshore flow; winds observed by sodar match synoptic pattern
8	**Included Case**
9	stationary front over WI/IL border at 15 and 18Z
11	**Included Case**
13	mixed layer does not develop; synoptic front almost directly above Zion at 12Z
15	**Included Case**
16	**Included Case**
17	omitted because of rain at Zion; mixed layer does not develop

With regards to the case of 12 June 2017: according to our criteria, the lake breeze front passed Sheboygan at 1543 UTC and Zion at 1730 UTC. Below is the surface map at 1500 UTC as analyzed by the NOAA Weather Prediction Center. A stationary front is present, but it is to the north of Sheboygan (identified with the red arrow). One might even claim that the boundary has been analyzed too far to the south, as the temperatures of locations just north of the front [like 85 F at La Crosse, WI (cyan arrow) and 84 F at Green Bay, WI (green arrow)] seem to have more in common with the conditions further to the south. In fact, note that Green Bay is actually warmer than Sheboygan at this time despite being further to the north, on the other side of the boundary, and the lack of maritime flow at Sheboygan. Importantly, the temperature drop and wind shift of the lake breeze are observed at Sheboygan within an hour of this analysis.

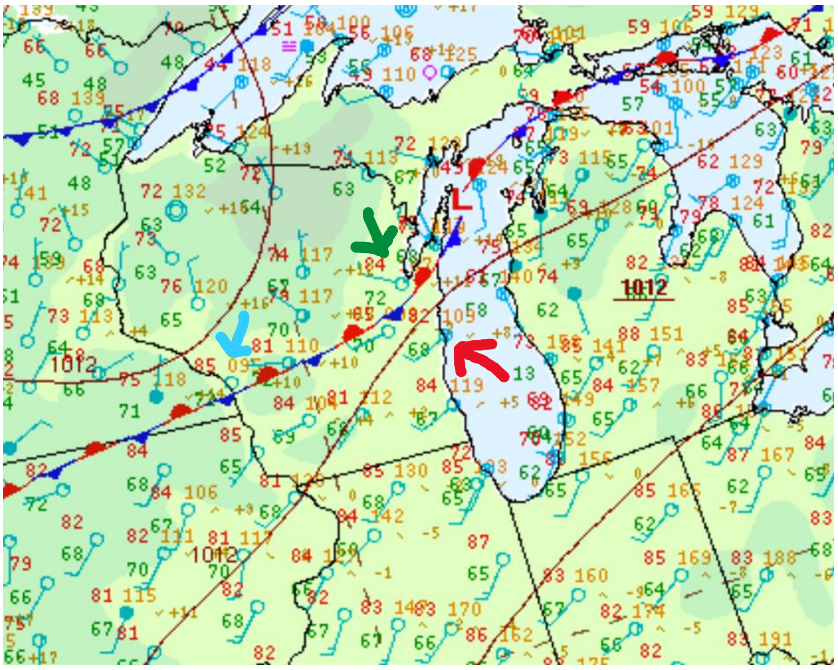

The next available surface chart is at 1800 UTC, near the end of our three hour window of analysis for Sheboygan. The analyzed boundary is closer to Sheboygan than it was before. However, we do not feel that the boundary propagation is responsible for the observed shift in winds. First, the pressure has actually risen at Sheboygan since the previous map even though the boundary has not yet arrived; one would expect to see the pressure dropping ahead of the frontal arrival and only begin rising after passage. Second, it is clear that along the coast of Lake Michigan, other lake breeze events are underway (witness the 20 F difference between the Chicago lakeshore and Midway airport, or the nearly 30 F difference between Milwaukee and the station just to its north). Were this a synoptically-impacted situation, those closely-paired stations would be under the same flow regime and thus display similar wind directions and temperatures.

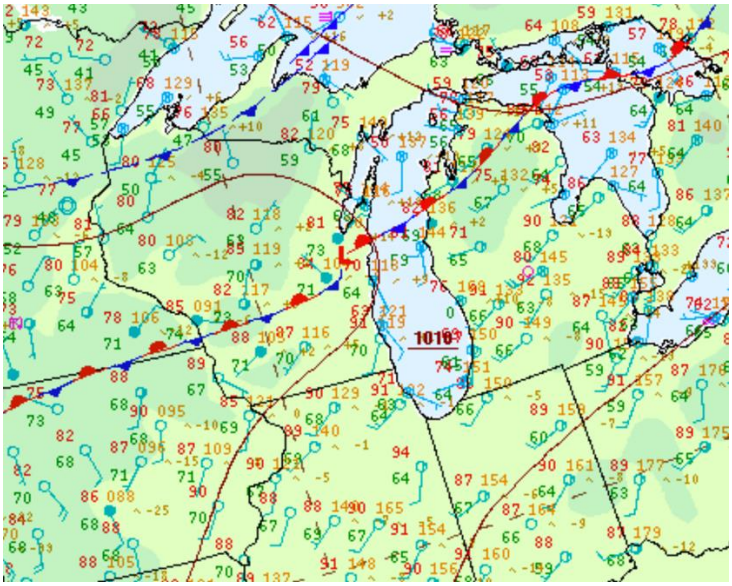

Perhaps of greatest relevance is the hourly evolution of conditions at the Sheboygan Airport (KSBM) in comparison to our shore-adjacent observations. As you can see from this map, the airport is relatively far inland (the large asymmetric X in the upper left). Our observation site is circled in the lower right. The airport is about 12 km from the shore at its closest, and slightly further than that to our site.

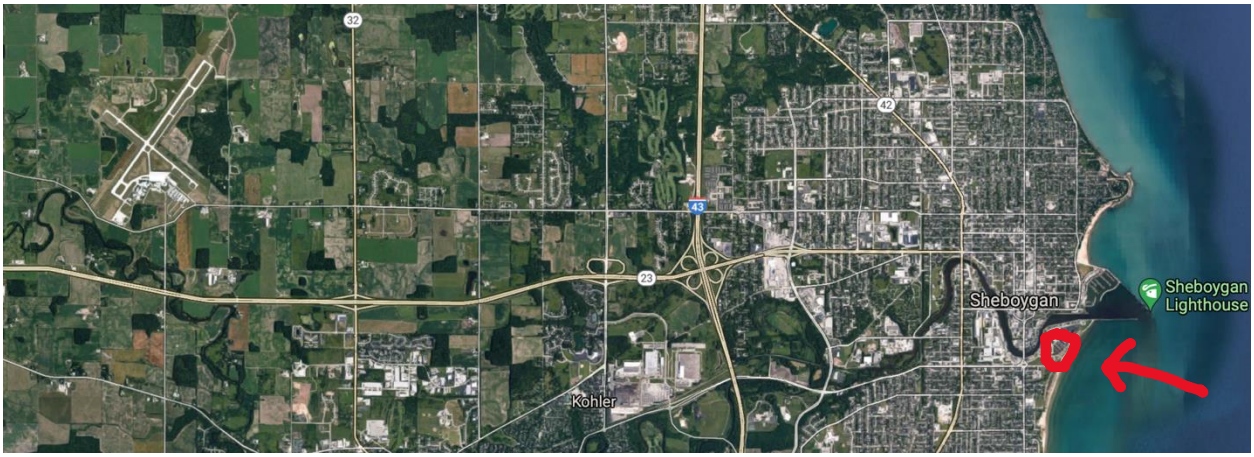

In the following table, we have obtained the hourly synoptic observations from KSBM and compared those to the 1 min observations we took at our observation site adjacent to the shore. (Honestly, it was fun putting my old METAR-decoding skills to use!) Wind directions are in degrees and temperatures are in C. Shore wind directions were available to the nearest 0.1 degree, but for this table, those values have been rounded to the nearest 10 deg to match the rounding of the ASOS observations. We have also included the inland-minus-shore differences. Hourly observations after 1543 UTC, the time we identified as the passage of the lake breeze front, are shaded.

Time (UTC)	KSBM Wind Dir	Shore Wind Dir	KSBM Temp	Shore Temp	Δ Dir	Δ T
1253	240	270	26.7	26.6	-30	0.1
1353	240	260	28.3	26.8	-20	1.5
1453	250	230	29.4	28.0	20	1.4
1553	270	190	28.9	22.8	80	6.1
1653	230	80	30.0	16.6	150	13.4
1753	220	140	30.0	14.7	80	15.3
1853	230	160	28.9	16.5	70	12.4

From the synoptic perspective, the 12 km distance between the airport and shoreline observations is small. They'd easily fit within the same GFS grid cell, for example. One would expect that the two locations would experience largely the same weather conditions due to synoptic influences. That is true through the 1453 UTC observations, with the two sites experiencing winds that are westerly or southwesterly and temperatures that are less than 2 C apart. However, after the 1543 UTC boundary passage, the conditions at the lake shore become remarkably different, both in terms of wind direction and temperature. If this were a synoptic boundary, we'd expect to see similar changes in the wind directions at the two sites more or less simultaneously. However, during the four hours of post-boundary observations the airport winds remain confined to the west or southwest while the shore winds swing all the way to the east; at 1553 UTC, for example, the winds at the two sites are nearly diametrically opposite. Simultaneously, the temperature at the airport increases while the temperature at the lake shore

drops substantially, resulting in a temperature difference that is ten times larger than it was before. In addition, this event was determined to be a near-shore event instead of an inland one which means the wind shift was not observed yet another station only 5.3 km from the shore. With only the near shore station experiencing wind and temperature shifts, and those shifts being consistent with the changes expected during and after the passage of the lake breeze front, we contend it is unlikely a synoptic scale boundary was responsible.

Zion was even further away from the purported synoptic influence. The boundary eventually began moving southward as a cold front, passing over Sheboygan sometime after 0000 UTC on the 13th. The low level winds observed by the Zion sodar are also inconsistent with the suggested S-SW to NE-NW shift that the synoptic boundary would cause:

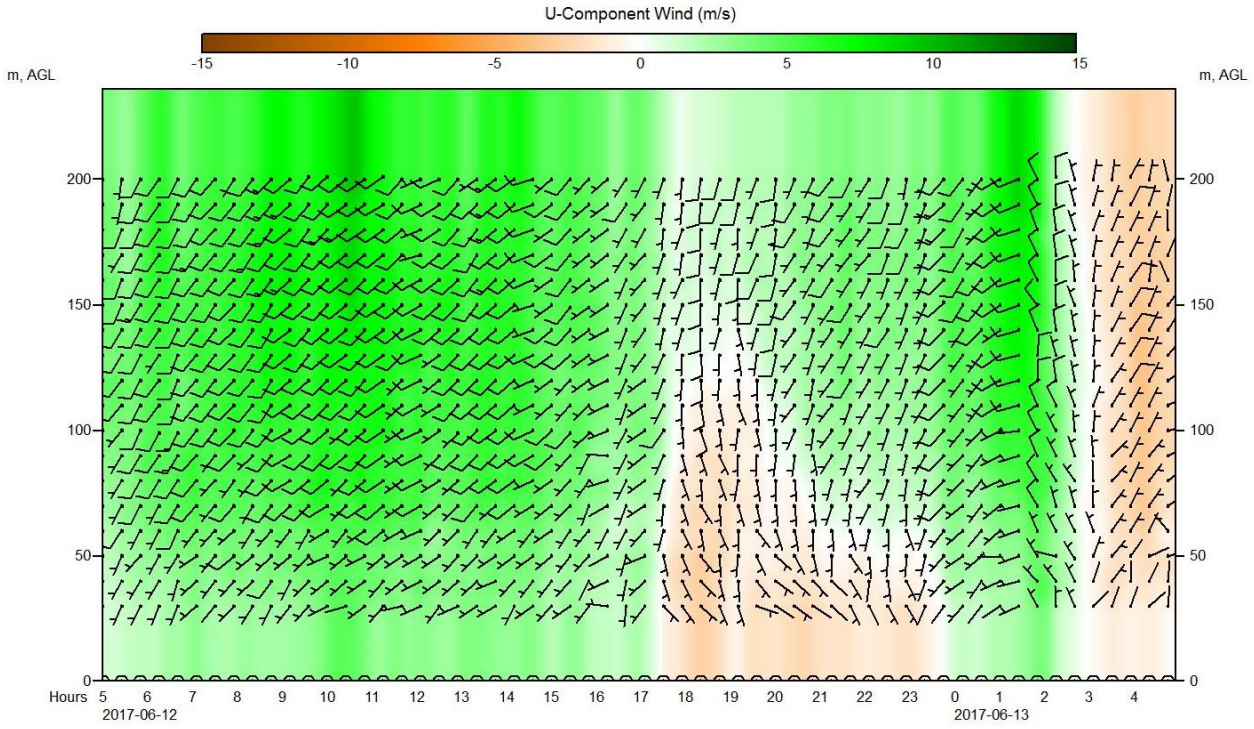

Our independent surface observations indicated the arrival of the lake breeze front at 1730 UTC. This is consistent with the low-level reversal in the u component of the wind shown in the figure above. According to these observations, the synoptic boundary may have arrived around 0130 UTC the next day when winds abruptly shift to the north over the entire observed column, but that is much too late to have had any influence on the lake breeze + 3 h period analyzed in this work.

Perhaps the most significant difference in criteria between our cases and that of the reviewer is that we elected to include mixing depth as a factor. The development of a well-defined mixed layer prior to lake breeze arrival is clear evidence that the air over the observation site is of continental origin in that the air temperature is being influenced by solar heating of the surface

and/or warm advection (which would be flow from the land and not the lake). A rapid collapse of this mixed layer would be corroborating evidence of lake breeze arrival, with air now being sourced off the lake. The resulting cold advection is strong enough to offset the solar heating, and surface temperatures decrease (another criterion we used to clearly identify lake breeze arrival). We feel that this adds an important dimension to the case selection. We have added a brief explanation as to why we included this criterion to the manuscript, and we have also added the following: "The cases chosen for analysis are a consequence of the selection criteria. While a set of more permissive criteria could result in a greater number of cases, events that are not unambiguously lake breezes might also be included."

Ultimately, during the preparation and revision of this paper, we carefully considered each and every day during the month-long LMOS deployment period. This includes the days that the reviewer believes we should have included or rejected. Through analysis of both the observations that were collected as part of this experiment as well as operational observations from the synoptic-scale network, we stand behind the cases we have chosen for analysis.

Detailed Comments
==========

L27 Abstract - 'Post-breeze' implies the wind direction after the lake breeze is over. I think instead you mean post-lake-breeze front, and thus during-breeze. Need to correct/clarify.

You are correct, and we have reworded this sentence to be more clear.

L36 Abstract - Again, this is confusing - should be 'the passage of the lake breeze front', or 'after the lake breeze arrives'

Again, you are correct, and we have made the suggested change.

L243 - 'two' should be 'one', no?

Our original wording treated Sheboygan and Zion separately in terms of numbers of events. Therefore 5 days had an event at both sites, for a total of 10 events, and the remaining two events only occurred at one site. We've reworded this to address the confusion.

L456 - Need a reference or two to support inland penetration distances of hundreds of kilometers. Sills et al. (2011) is one.

We have added a citation to Sills et al. (2011).

L506 - Could these be standing waves generated by synoptic-scale near-surface flow encountering a 'ridge'? With the ridge being the lake-breeze front. I think this effect is mentioned in Segal et al. 1997.

The 3 near-shore cases were characterized by a) patterns of MSLP that would produce southwesterly flow near the surface, and b) relatively strong southwesterly flow at 850 hPa. Generally, the 3 inland cases had a weaker MSLP pattern and, more apparent, weaker flow at 850 hPa. Using the 'standing wave' argument, one could expect an alternating pattern of vertical velocities in both the near-shore and inland cases, but the pattern would likely be more pronounced with the near-shore cases (because of the stronger synoptic flow) as observed by the sodar. Note, we don't necessarily see a discussion on this topic in Segal and we don't recall having read it elsewhere in the literature (though we are not claiming that it is an original idea). We have added a brief discussion on this to the manuscript.

L516 - But this doesn't say anything about the periodicity, which was introduced and should be explained.

We hope that the explanation above sheds some light on this topic.

L590 - Should be 'the air temperature over the lake'.

While we intended to address the temperature of the lake surface here, it is now apparent that it could be confusing to refer to the continental air temperature in the same clause as the water temperature. Therefore, we have made the suggested change.

L616 - Need to say that due to small sample size this evolution may not be representative of most lake breezes cases, particularly in different regions of the Great Lakes with different lakeshore geometries.

We added some text to the last paragraph noting that observations at different locations are required.

Reviewer #3

The structure of the revised version (i.e., Section 4) has been greatly improved, which makes reading much easier. I do not have more scientific questions now. The manuscript is suggested to be accepted by JAS for publication after a minor revision

We are happy and grateful that you are pleased with both the science and the readability of this paper. We thank you for embarking with us on this journey.

1) Section 2, Part b, Instrumentation. I should ask this question in the previous review(s). I do still feel that the description of instrumentation seems has too many details given the focus of this study. To me, Table 2 is sufficient to know the instrumentation. It will be helpful if the authors can simplify the description of instrumentation slightly. For instance, I am not sure how many readers are interested in so detailed description of instrumentation as presented in Lines 198-201 and L204-209.

There are multiple audiences for this paper. The paper is primarily written for those who are interested in learning more about lake breeze properties and processes. However, the remote sensing community will read this paper to see novel applications of their instrumentation and techniques, and they will be interested in that level of detail. That being said, we have removed some of the specific details to make the instrumentation section slightly easier to read.

2) L182: The a priori temperature … I am not sure that you need "the" here.

The remote sensing community typically uses the phrase “a priori” (literally, “from what comes before”) as an adjective or noun that describes the mean state of the atmosphere and its covariance. Therefore, it is not uncommon to see or hear the phrase “the a priori state” or even “the a priori.” For example, the seminal Rodgers (2000) text on optimal estimation says, “[o]nce a large set of remote measurements has been made, it may be possible to use them to improve on the *a priori* to be used for future retrievals.” (italics in original).

3) L244: It is not clear the difference between local time and LST (Local Standard Time). In addition, please make sure that LST is defined at its first use.

We include three measures of time in this sentence with the knowledge that different user communities typically are interested in different times. Many scientists are accustomed to working in UTC, but that says little about what is happening relative to the sun. Local Standard Time tells us what is happening relative to the sun, but it is an hour offset from the clock on the wall due to daylight saving time. LST is especially important to air quality scientists and others who work with diurnal cycles that are governed by the sun, and many observations in that community are recorded in LST instead of local time or UTC. Local time perhaps has the least scientific utility, but it is the most important for anyone who just want to know what time the temperature is going to drop. We include all three times here, with the knowledge that from then on readers will be able to make their own conversions themselves. Since we only use LST

twice, we have just expanded the acronym in both instances. Thank you for drawing our attention to that oversight.

4) L279: "were" should be "are" for consistency with another "are" in the same sentence?

We have just changed it to "…the mean winds at Zion are over 1.4 times faster after LBA than before" to remove the issue entirely.

5) L303-308: Any explanation of a decrease in mixing ratio with LBA at Sheboygan site? Is it because of less evaporation with lower lake surface near this site?

We assume you mean lower lake surface temperature. That is exactly correct and we have made that connection explicit in the manuscript.

6) L350: brings with it □ bring with. Please delete "it" if I do not misunderstand.

We have changed this to "results in"

7) L456: "extend hundreds of kilometers inland". Here "hundreds of kilometers" seems to be too many for Lake Breeze traveling inland unless the authors may provide reliable reference(s).

Reviewer #1 had the same concern, which we have addressed.

8) I am not sure that you need to add dot in all the panel labels in Figures 2-4, and 6-7. For instance, "a)" should be more commonly used than "a.)"?

The lead author has typically used the letter-period-parenthesis notation (see https://doi.org/10.1175/JTECH-D-20-0182.1 for an unrelated example) and previously has not received comments from reviewers or editors on the issue. If we needed to re-render the figures in order to correct scientific errors, readability concerns, or other issues raised by the reviewers, we would likely make the change suggested by the reviewer. However, with no other changes suggested by either reviewer for any of the figures, we feel that it is not necessary to redo several figures to address a small stylistic difference.

Observations of the Development and Vertical Structure of the Lake Breeze Circulation During the 2017 Lake Michigan Ozone Study

Timothy J. Wagner[1], Alan C. Czarnetzki[2], Megan Christiansen[3], R. Bradley Pierce[1,4], Charles O. Stanier[3], Angela F. Dickens[5], and Edwin W. Eloranta[1].

1. Cooperative Institute for Meteorological Satellite Studies (CIMSS), Space Science and Engineering Center (SSEC), University of Wisconsin – Madison, Madison, Wisconsin

2. Department of Earth and Environmental Sciences, University of Northern Iowa, Cedar Falls, Iowa

3. Department of Chemical and Biochemical Engineering, University of Iowa, Iowa City, Iowa

4. Department of Atmospheric and Oceanic Science, University of Wisconsin – Madison, Madison, Wisconsin

5. Lake Michigan Air Directors Consortium (LADCO), Hillside, Illinois

Corresponding author: Timothy J. Wagner, tim.wagner@ssec.wisc.edu

Abstract

Ground-based thermodynamic and kinematic profilers were placed adjacent to the western shore of Lake Michigan at two sites as part of the 2017 Lake Michigan Ozone Study. The southern site near Zion, Illinois, hosted a microwave radiometer (MWR) and a sodar wind profiler, while the northern site in Sheboygan, Wisconsin, featured an Atmospheric Emitted Radiance Interferometer (AERI), a Doppler lidar, and a High Spectral Resolution Lidar (HSRL). Each site experienced several lake breeze events during the experiment. Composite time series and time/height cross sections were constructed relative to the lake breeze arrival time so that commonalities across events could be explored.

The composited surface observations indicate that the wind direction of the lake breeze is consistently southeasterly at both sites regardless of its direction before the arrival of the lake breeze front. Surface relative humidity increases with the arriving lake breeze, though this is due to cooler air temperatures as absolute moisture content stays the same or decreases. The profiler observations show that the lake breeze penetrates deeper when the local environment is unstable and pre-existing flow is weak. The cold air associated with the lake breeze remains confined to the lowest 200 m of the troposphere even if the wind shift is observed at higher altitudes. The evolution of the lake breeze corresponds well to observed changes in baroclinicity and calculated changes in circulation. Collocated observations of aerosols show increases in number and mass concentrations after the passage of the lake breeze front.

1. Introduction

It is well known that the Laurentian Great Lakes have a significant impact on the weather and climate of the upper Midwestern United States. These large bodies of water (which collectively encompass approximately 18% of the world's supply of liquid freshwater) force changes in temperature, cloud cover, and precipitation with significant diurnal and seasonal variability (Scott and Huff 1996), and the impacts of the lakes can even extend to severe convective weather (King et al. 2003). The lake breeze circulation is one of the most important mechanisms for latent and sensible heat exchange between the lakes and the surrounding environment. This is, in part, due to common occurrence of the Great Lakes lake breezes. For example, Laird et al. (2001) constructed a 15-year climatology of Lake Michigan lake breeze events and found that lake breezes tended to occur more frequently as the summer progressed. Depending on the location, lake breeze frequency increased from 5 to 9 events per month in May to 8 to 12 per month in August. Other studies have used different criteria to identify lake breezes and found higher frequencies. Lyons (1972) showed that Chicago, Illinois, experienced a lake breeze on approximately half of all days in May through September. With events occurring multiple times a week during the warm months, operational forecasters need to be familiar with their formation, structure, and impacts, while numerical weather prediction and air quality models must be able to simulate them properly.

Since a substantial fraction of the world's population lives in coastal regions, sea and lake breezes have been a subject of interest to humanity since antiquity (Simpson 1994, Miller 2003) and the broad outlines of their formation have been known for generations. Due to water's large heat capacity, its ability to absorb solar energy over a finite depth, and the vertical mixing present

in large bodies of water, surface temperatures respond slowly to solar heating. On the seasonal timescale, peak lake surface temperatures lag their terrestrial counterparts by several weeks while on diurnal scales lake temperatures are typically colder than land during the day but warmer at night. As a result, a sharp land-water gradient in the temperature and density of the near-surface air can arise, inducing a circulation as the atmosphere attempts to restore equilibrium. This circulation is commonly found where the body of water has sufficient thermal mass relative to the land. While the sea breeze and Great Lakes breezes are well known, lake breezes have also been observed for both natural lakes and reservoirs with length scales of just a few km (Segal et al. 1997).

A robust solenoidal-based explanation of the lake breeze circulation has emerged (Holton 1992, Miller et al. 2003, Martin 2006). The Bjerknes circulation theorem states that the material (Lagrangian) change in the absolute circulation C_a of a fluid element can be described as:

$$\frac{dC_a}{dt} = -\oint \frac{dP}{\rho} \qquad (1)$$

where P is pressure and ρ is density. In the special case of a barotropic fluid, density is a function of pressure alone and the right-hand side reduces to the closed line integral of an exact differential (which is zero). Thus, Bjerknes's circulation theorem is merely a more general case of Kelvin's circulation theorem, which states that the absolute circulation in a barotropic fluid is conserved. However, the differential heating present at a lake or sea boundary ensures that the environment is far from barotropic: the daytime geopotential heights are greater over the land, and thus isobars slope downward toward the cooler water while isopycnals (lines of constant density) slope toward warmer land. This ensures that the environment is baroclinic. The horizontal flow both at the

surface and aloft is isobaric and does not contribute to the circulation change, as $dp = 0$ for those branches. However, as the daytime ascending branch (over land) and the descending branch (over water) are associated with environments with very different densities, there is a net difference between these two branches and thus an acceleration along the perimeter of the fluid element is induced. This is a thermally direct circulation, and over time the vertical motions would be expected to reduce the baroclinicity of the environment as the isopycnals would be rotated to be more parallel to the isobars. At night, a weak land breeze can develop when the temperature gradient is reversed.

Changes in the thermodynamic structure of the environment would clearly be expected to accompany the changes in the kinematics described above. The development of onshore flow at low levels produces cold air advection. The flow of this comparatively denser air from water to land takes the form of a localized gravity current (Miller et al. 2003). The cooler air inhibits convection, producing clearing skies that can be seen on satellite imagery; a characteristic example of this is depicted in Figure 1. Since temperatures above the gravity current are not affected, a shallow inversion will develop (Keen and Lyons 1978).

The present study comprehensively describes the temporal and vertical development of the lake breeze circulation on the western shore of Lake Michigan using data collected during the 2017 Lake Michigan Ozone Study (LMOS 2017, Stanier et al. 2021). The development and structure of western Lake Michigan breezes have been of considerable interest for many (e.g. Lyons 1972, Keen and Lyons 1978, Sills et al. 2011), likely due in part to the large population centers located along the lake shore. One aspect of the relationship between these major urban areas and the lake is the adverse impacts that lake breezes have on air quality, as they have been shown to play a significant role in the production and transport of ground-level ozone in shoreline communities

along Lake Michigan (Lyons and Cole 1976, Dye et al. 1995, Levy et al. 2010). Ozone precursors emitted from densely populated regions are transported over the lake. So long as the precursors remain offshore, the shoreline communities are not impacted by increased ozone production. When the lake breeze is present, however, ozone and its precursors are transported inland and convergence along the lake breeze boundary results in significant increases to observed ozone concentrations. The deployment of high-temporal resolution thermodynamic and kinematic profilers alongside aerosol lidars, air samplers, and other instruments, at two sites adjacent to Lake Michigan in support of LMOS 2017, allows the investigation of lake breeze events from a novel perspective. While other studies have investigated the kinematic characteristics of lake and sea breezes using higher-temporal resolution profiling instruments like Doppler lidars (e.g., Curry et al. 2017, Banta et al. 1993) and sodars (e.g., Mastrantonio et al. 1994, Prakash et al. 1992), the present work introduces continuous thermodynamic profiling using instruments observing both microwave and infrared emission. When coupled with collocated wind profiling instruments, a detailed picture of the thermodynamic and aerosol characteristics of the lake breeze circulation and its evolution emerges. Wind and thermodynamic profiles from lake breeze events are composited on an event-centric time scale to capture the behavior of the atmosphere before and after lake breeze arrival; a similar technique has been used to investigate the near-storm environment of severe storms (Wagner et al. 2008) and bores (Loveless et al. 2019). The remainder of this paper describes the field campaign and the instruments (Section 2), explores the evolution of surface weather conditions (Section 3), vertical structure (Section 4), and particulate air quality (Section 5), and synthesizes these observations to improve understanding of lake breeze circulations from the combined thermodynamic and kinematic perspective (Section 6).

2. Measurements and Instrumentation

a. The 2017 Lake Michigan Ozone Study

The 2017 Lake Michigan Ozone Study (LMOS 2017) was devoted to observing chemical and meteorological features important to persistently high ozone concentrations along the western shore of Lake Michigan. Project collaborators included NASA, NOAA, EPA, the Lake Michigan Air Directors Consortium (LADCO), state environmental agencies, universities, and the private sector. A significant goal of LMOS 2017 was to better understand how the unique geography and meteorology of the Lake Michigan basin drives significant ground-level ozone production even in communities with relatively low emission rates of ozone precursors. By uniting land-based, ship-based, and airborne measuring systems, a comprehensive portrait of the thermodynamic, kinematic, and chemical state of the coastal environment during high ozone events was obtained. An additional goal of the experiment was to use the data to evaluate the performance of meteorological and air quality models and inform their improvement.

The field phase of LMOS 2017 was conducted from 22 May to 22 June 2017. This period historically encompasses a significant number of ozone exceedance events for shoreline communities due to the combination of numerous lake breeze events (as the lake has not yet warmed significantly) coupled with sufficient insolation to induce the photochemistry required for ground level ozone production; the cold water also inhibits mixing and ensures that precursors remain near the surface. Two ground-based supersites were established. The more southerly supersite was near Zion, Illinois (roughly halfway between Chicago and Milwaukee). The northern supersite was at Sheboygan, Wisconsin (about 80 km north of Milwaukee); a map depicting their locations is seen in Figure 1. The Sheboygan site (43.745 N, 87.709 W) was within 230 m of the shore while the Zion site (42.468 N, 87.810 W, AQS 17-097-1007) was approximately 1 km

inland. The lake shore has a similar north-south orientation in the vicinity of the two sites, although the shoreline is more sinuous at Sheboygan. In-depth descriptions of the two sites are found in Doak et al. 2021. Airborne platforms included the NASA UC-12, which carried remote sensing instruments for aerosols, clouds, and trace gases, and a light aircraft operated by Scientific Aviation, which conducted in situ profiling of trace gases and meteorological characteristics. The NOAA research vessel R5503 provided near-shore transects of surface meteorology and trace gas concentrations with a Pandora differential absorption optical spectrometer (Herman et al. 2009), while on-shore vehicles conducted mobile sampling of terrestrial ozone and meteorology. Preliminary campaign results have been reported (Abdioskouei et al. 2019, Vermeuel et al, 2019) and analysis of this significant volume of data is ongoing.

b. Instrumentation

For the purposes of the present work, the most significant data were collected at the two supersites near Sheboygan and Zion. The Space Science and Engineering Center (SSEC) Portable Atmospheric Research Center (SPARC, Wagner et al. 2019) was deployed at Sheboygan, while a Radiometrics MP3000 and an Atmospheric Systems Corporation acoustic wind profiler, or sodar, were deployed at Zion. Surface observations at the two sites came from instruments mounted on 10 m towers, and each site also featured air quality instrumentation to measure ozone and particulate matter.

SPARC, a portable ground-based atmospheric profiling laboratory, includes an Atmospheric Emitted Radiance Interferometer (AERI, Knuteson et al. 2004a, 2004b), a Halo Photonics Stream Line XR Doppler lidar (DLID, Pearson et al. 2009), and a High Spectral Resolution Lidar (HSRL, Shipley et al. 1983, Eloranta 2005). The thermodynamic state is captured

by AERI, a commercially-available hyperspectral infrared radiometer that passively measures downwelling near- and thermal infrared spectra with a spectral resolution better than 1 cm^{-1} and a temporal resolution of approximately 30 s. Profiles of temperature and water vapor can be retrieved from AERI-observed spectra through the Tropospheric Remotely Observed Profiling via Optimal Estimation (TROPoe) retrieval, formerly known as AERIoe (Turner and Löhnert 2014, Turner and Blumberg 2019). TROPoe profiles have been shown to agree well with radiosondes when they originate from either an AERI (Turner and Löhnert 2014, Turner and Blumberg 2019) or an MWR (Turner and Löhnert 2021). The a priori atmospheric state for the retrieval during this deployment was calculated from a multiyear climatology of late spring and early summer radiosondes launched from the National Weather Service office at Green Bay, Wisconsin. A principal component analysis noise filter is applied to the AERI radiances to reduce noise before the retrieval is applied, in which the observations are decomposed into principal components and the spectrum is rebuilt from those that have the greatest variance (Turner et al. 2006). The DLID uses a 1.5 μm pulsed laser to capture the radial velocity of boundary layer aerosols; by scanning at a fixed zenith angle at different azimuths, it is possible to geometrically calculate the wind profile above the lidar. The HSRL is a vertically-pointing lidar that uses spectral width differences to discriminate between molecular and aerosol scattering: the spectrum for aerosol backscattering is confined to the relatively narrow range of Doppler-shifted frequencies associated with vertical motions in the atmosphere while the molecular spectrum is broadened by the Maxwellian thermal motion of the molecules. This allows high-precision absolutely-calibrated aerosol backscatter retrievals and independent retrievals of aerosol extinction. With these instruments, SPARC is able to provide a comprehensive profile of the evolution of the atmospheric state on a time scale that is measured on the order of minutes.

198 At Zion, the MWR passively observed the brightness temperature of downwelling radiance
199 in 22 channels, with eight channels measuring the water vapor absorption band and 14 channels
200 observing the oxygen absorption band. The TROPoe algorithm was then used to retrieve profiles
201 of water vapor and temperature from these measurements using the same prior data as were used
202 for the Sheboygan retrievals; by using TROPoe instead of the manufacturer-supplied neural
203 network retrievals, a more direct comparison to the AERI observations at Sheboygan could be
204 carried out. The sodar operates at audio frequencies near 4500 Hz, emitting a high intensity
205 acoustic pulse and sampling the atmospheric echo. The frequency of the echo is directly
206 proportional to the radial motion of the scattering volume relative to the instrument. The radial
207 motions determined from the Doppler shift of each pulse in a set are combined to produce three-
208 dimensional wind profiles from 30 to 200 m above ground level (AGL).

209 The Zion site was also home to several air quality instruments. A Scanning Mobility
210 Particle Sizer and Aerodynamic Particle Sizer (SMPS-APS, Shen et al. 2002) system measured
211 aerosol size distributions at the surface, covering a combined aerodynamic diameter size range of
212 13 nm – 8354 μm. The size distributions from the APS were converted from aerodynamic to
213 electrical mobility diameters (SMPS) and merged to the final size distribution following the
214 method presented in Khlystov et al. (2004). Size distributions were averaged to a common 10-min
215 time series. An Aerosol Robotic Network (AERONET, Holben et al. 1998) measuring aerosol
216 optical depth (AOD) was also located at the Zion site from June 4 – June 22 of the campaign.
217 AERONET level 2.0 data (cloud screened and quality assured) are used in the present work
218 (Smirnov et al. 2000). AOD was interpolated to 550 nm in the following manner:

219 $$\tau_{\lambda_{550}} = \tau_{\lambda_{500}} \left(\frac{\lambda_{550}}{\lambda_{500}}\right)^{-\alpha} \quad (2)$$

where $\tau_{\lambda_{500}}$ is AOD at 500 nm and α is the angstrom exponent (440-870 nm) as reported by AERONET. The relevant characteristics of the instruments used in this study are summarized in Table 1.

c. Lake breeze events

The following criteria were used to objectively identify the lake breeze events (defined as the passage of a lake breeze front) at the two sites:

1. The zonal (u) component of the surface wind reversed from offshore to onshore.
2. Surface temperatures dropped abruptly with the wind shift.
3. Mixing height decreased with the wind shift.
4. No rain was detected within three hours of the wind shift.

The cases chosen for analysis are a consequence of the selection criteria. While a set of more permissive criteria could result in a greater number of cases, events that are not unambiguously lake breezes might also be included. The mixing height criterion was included to establish that the atmospheric environment before the lake breeze was continental in character, with the air temperature being influenced by solar heating and/or warm air advection. A decrease in the mixing height coincident with the wind shift indicates that surface air is now originating over the lake. Laird et al. (2001) identified a set of criteria to objectively identify lake breeze, including a change in wind direction, maximum air temperatures greater than that of the lake surface, and synoptically quiescent conditions. While the Laird et al. (2001) criteria were not specifically used as filtering criteria in the present study, all of the lake breeze events examined here also satisfied these criteria.

The identification criteria were applied separately to the Sheboygan and Zion observations, and the time of the lake breeze arrival (LBA), representing the moment the lake breeze front passed

over the observing sites, was defined as the time of the greatest shift in wind direction. This resulted in a total of six lake breeze events at each location, consistent with the climatology for late spring (Laird et al. 2001). Five study days included lake breezes at both sites while two days had an event at only one site and not the other. On average, LBA occurred much earlier at Sheboygan (1541 UTC, 10:41 AM local time, 9:41 AM local standard time) than Zion (1630 UTC, 11:30 AM local time, 10:30 AM local standard time). However, the small number of cases and variability in arrival times at each site means this difference is not statistically significant. For the five days in which lake breezes were observed at both locations, the correlation in LBA was low ($r=0.0935$). The lack of correlation between arrival times is consistent with an understanding that lake breeze events are driven more by local conditions than by synoptic forcing. Analysis of contemporaneous surface maps helps illustrate this last point: in all cases, any synoptic scale disturbances were either hundreds of km removed from the observing sites, were stationary, or did not propagate over the observation domain until after the period analyzed in this paper. The dates and times of the observed lake breezes are shown in Table 2.

3. Composite Surface Conditions

An objective method to identify the timing of lake breeze events was used to composite the individual cases observed during the LMOS 2017 campaign. For each event, the time of LBA was subtracted from the observation times so that the resulting timeline was measured relative to LBA. The observations from each instrument and event were then interpolated to a common timeline with 5 min resolution from 3 h before LBA to 3 h after; this facilitated comparisons across instruments and events. Figure 2 illustrates the results of this composite analysis for the surface conditions at the two sites. Results from Sheboygan (Zion) are shown with solid (dashed) lines.

Thin colored lines represent individual events while thick black lines represent the mean of all events for a particular site. The mean wind speed and direction were calculated by first determining the mean zonal (u) and meridional (v) components of the wind, then converting to speed and direction. Overall, surface conditions are consistent with what would be expected during a lake or sea breeze event, but there are some interesting details. Panel 2a exhibits the wind directions for the various events, with the wind shift used to define LBA clearly evident. Both sites have nearly identical time series for the mean wind direction, with westerly winds undergoing a rapid shift to southeasterly at LBA followed by a much slower turning towards a more southerly direction over the ensuing hours, a result of Coriolis (inertial) acceleration. Substantial variations from one event and site to the next can be seen prior to LBA, but once the lake breeze front has passed the wind directions are much more uniform. This lower variability in wind direction may be due to consistency in the onshore perturbation horizontal pressure gradient force that develops as the air over land warms, and the reduced friction surface winds experience flowing over water. The wind speed (Figure 2b) shows substantial variability between cases and from one time step to the next. On average, the speeds are higher at Zion than Sheboygan, and while Sheboygan has little change in the mean wind speed pre- and post-LBA, the mean winds at Zion are over 1.4 times faster after LBA than before.

While the driving factor of the lake breeze circulation is the difference between the temperatures of the air over land and water, the lack of observations of the latter means that the lake surface temperature needs to be used as a proxy. Figure 2c shows the time series for the difference between the air and lake temperature on lake breeze days. In situ observations of the lake temperature are sparse, with no operational buoys within tens of km of Sheboygan. Therefore, lake surface temperatures were obtained from the Great Lakes Research Laboratory (GLERL)

289 Great Lakes Surface Environmental Analysis (GLSEA, Schwab et al. 1999). Values were obtained
290 from the GLSEA grid points located approximately 10 km from the observation sites at an azimuth
291 of 140 degrees (the average wind direction 1 h after LBA). The analyses are computed once per
292 day, and these temperatures are recorded in Table 2. On average, the lake at Zion is about 3 °C
293 warmer than near Sheboygan, and during the month-long experiment seasonal warming caused a
294 greater increase at Zion. On average the air/lake temperature difference (Figure 2c) gradually but
295 steadily increases at a rate that is effectively identical for both locations. Following LBA, the mean
296 lake/land difference decreases substantially at Sheboygan, dropping from 12.2 °C at LBA to 3.2
297 °C just one hour later. A smaller change is observed at Zion, as the mean air/lake temperature
298 difference goes from 12.1 °C to 9.7 °C during the same period. The overall pattern for ambient
299 air temperature is largely the same as the air/lake differences (not shown). Air temperatures at Zion
300 tended to be warmer than at Sheboygan both before and after LBA, a function of Zion's lower
301 latitude, a longer fetch over land to reach the observing site, and lake breezes that occurred later
302 in the day allowing more solar heating before LBA. Absolute water vapor content (as represented
303 by the mixing ratio, Figure 2d) shows a very gradual increase in the hours before LBA consistent
304 with typical evolution of the planetary boundary layer (PBL). The lake breeze itself has very little
305 impact on the mixing ratio at Zion for any event, but four of the six Sheboygan events experience
306 a notable decrease in mixing ratio with LBA. This can be explained by the relative differences
307 between the lake air and land air temperatures at the two sites: Zion had a much smaller difference
308 than Sheboygan, so there was little difference between the saturation mixing ratios following LBA.
309 By contrast, Sheboygan experienced a significant decrease in its saturation mixing ratio following
310 LBA due to the colder air temperatures, and so absolute water vapor content decreased even though
311 the arriving air originated over a large body of water. By contrast, the relative humidity at both

312 sites (not shown) showed an increase following LBA. Since the absolute humidity was constant or
313 decreasing following LBA, this increase in relative humidity was solely driven by the decrease in
314 air temperature.
315
316 **4. Composite Vertical Structure**
317 It is well known that the structure and influence of the lake breeze circulation extends
318 vertically beyond the near-surface level. Previous studies have used frequent balloon launches
319 (Lyons 1972), instrumented aircraft (Finkele 1995), and kinematic profilers (e.g. Curry et al. 2017,
320 Banta et al. 1993) to investigate the vertical structure of lake breeze circulations. However,
321 continuous contemporaneous observations of winds, temperature, and moisture profiles during
322 lake and sea breeze events have been rare. LMOS 2017 provided a unique opportunity to assess
323 how the vertical structure of these fields evolved over time during several different lake breeze
324 events. Here, the same compositing technique described earlier is applied to the vertical dimension
325 so that structure in the PBL can be resolved. An important caveat when looking at the vertical
326 plots of remotely-sensed thermodynamic variables is that the true vertical resolution (that is, the
327 minimum size of an element that can be resolved by the profiler) is finer for an infrared than a
328 microwave radiometer due to the narrower weighting functions and higher information content
329 found in the infrared band (Ebell et al. 2013, Blumberg et al. 2015). The TROPoe retrieval can be
330 used to quantify how well each instrument resolves both temperature and water vapor structure.
331 On average, at the 200 m level (which is roughly the height of the post-LBA inversion), the AERI
332 vertical resolution for temperature was approximately twice as fine as the MWR (0.25 km and 0.49
333 km respectively) and was approximately 2.5 times better for water vapor (1.19 km and 3.00 km
334 respectively). Therefore, the enhanced detail visible in the Sheboygan time-height cross sections

335 of thermodynamic variables is far more likely to be due to the differences in the instruments used
336 than physical differences in the lake breeze itself.
337
338 *a. Temperature and Moisture Structure*
339 Time-height cross sections of temperature and mixing ratio overlaid with wind barbs are
340 shown in Figure 3. Observations from all instruments were interpolated onto a common grid with
341 temporal resolution of 5 min (same as the surface composites shown earlier) and a vertical spacing
342 of 20 m. The data from both Zion and Sheboygan illustrate that while the increase in temperature
343 in the period leading up to LBA is greatest at the surface, increases in temperature with time are
344 seen several hundred meters above the surface as the surface air is mixed upward. There is an
345 inversion present a few hours before LBA that is more easily seen in Sheboygan than Zion. There
346 are two reasons for this: first, since the average time of LBA is earlier at Sheboygan, the three-
347 hour period preceding LBA is more likely to include an early-morning inversion; and second,
348 enhanced vertical resolution enables the AERI to resolve the inversion with increased fidelity.
349 Prior to LBA winds near the surface are southwesterly and are veering with height, becoming
350 northwesterly at an altitude of 1 km. Wind direction at a given height tends to be constant with
351 time before LBA, though there is a tendency for the speeds to decrease with time. In the 30 min
352 prior to LBA, the potential temperature gradient in the lowest 400 m (not shown) is greatly relaxed
353 as the lower troposphere undergoes significant mixing while the free troposphere remains largely
354 adiabatic both before and after LBA. The arrival of the lake breeze results in a sudden decrease in
355 temperature that is greatest at the surface but still prevalent in the lowest 100 – 200 m; again, this
356 is more evident in the AERI observations. A strong inversion develops post-LBA as the cold lake
357 air advances beneath and lifts the warmer land air. Strong marine inversions such as these are

358 expected in the spring when the lakes are significantly colder than the nearby land. Above the
359 inversion, the air temperature at a given height increases with time. This is likely subsidence-
360 induced warming, caused by the descending branch of the lake breeze circulation, which helps to
361 enhance the strength of the inversion and increase the stability of the environment. Therefore, the
362 cold temperatures commonly associated with the lake breeze are confined to a shallow layer in the
363 lowest part of the troposphere even as the breeze-induced changes in wind direction extend above
364 that height. Figure 3 also shows the mixing height calculated from the composited thermodynamic
365 profiles. Mixing height grows throughout the morning with increased diabatic heating, and is
366 deeper at Zion where air temperatures are warmer. However, the arrival of the lake breeze causes
367 a sudden drop in the mixing height as the atmosphere rapidly stabilizes. This has significant
368 ramifications on air quality, as the lake breeze circulation-induced inversion traps ozone precursors
369 and other pollutants in the near-surface air (Dye et al. 1995, Levy et al. 2010).

370 These observations show a disconnect between the depth of cold air and the depth over
371 which the lake breeze circulation is impacting wind direction. The depth of the cold air that arrived
372 onshore is limited by the vertical extent of conductive cooling. Both observations and numerical
373 simulations indicate that significant heat loss by conduction is limited to the lowest 150 m of the
374 atmosphere (Lyons 1970). However, winds are clearly changing above the cold pool. Before LBA,
375 westerly surface winds indicate the synoptic scale horizontal pressure gradient force is directed
376 toward the northeast. With sunrise, the near-surface air over land warms more rapidly with solar
377 heating, producing a perturbation horizontal pressure gradient force directed onshore. In
378 combination with the synoptic scale horizontal pressure gradient force, this produces an
379 ageostrophic southeasterly surface wind at LBA. Observations over land indicate the warming
380 eventually continues above the cold layer, but is delayed after collapse of the mixed layer resulting

from LBA at the surface. It is likely this upper warming over land is greater than above the lake. As a result, the onshore perturbation horizontal pressure gradient force also develops at upper levels, but later than at the surface. Therefore, one would expect a delay in the arrival of southeasterly winds at higher levels and a gradual upward slope to the advancing lake breeze front.

Vertical profiles of the water vapor mixing ratio are also displayed in Figure 3. It can be challenging to interpret remotely-sensed profiles of moisture as the information content present in the infrared and microwave spectra for moisture is less than for temperature. Consequently, the vertical distribution of water vapor is not as clearly resolved as is temperature. Due to these limitations it is likely that vertical gradients in moisture are actually greater than what is shown. Still, valuable insight can be obtained by inspecting the observations. Mixing ratio profiles at Sheboygan show markedly lower values than at Zion, which is consistent with the surface observations. However, due to the lower temperature at Sheboygan, the relative humidity values (not shown) are of similar magnitude at the two sites. In the hours before LBA, warming-induced evaporation likely explains the observed increase in mixing ratio; simultaneously, the relative humidity is constant/decreasing with time as the effect of increased water vapor on relative humidity is outpaced by the higher temperatures. Following LBA, the mixing ratio observations in the lowest level of the profiles at the two sites are consistent with the values reported by the surface observations: nearly constant at Zion and slightly decreasing at Sheboygan.

The sodar and Doppler lidar are clearly resolving the lower branch of the lake breeze circulation. What is not clearly evident in these figures, however, is the presence of the upper level return flow. While the 200 m vertical range of the Zion sodar is likely too shallow, conceivably the lidar at Sheboygan could observe it since aircraft observations of a sea breeze by Finkele et al. (1995) showed return flow occurring between 700 and 1000 m. With easterly surface

winds at Sheboygan post-LBA one would expect corresponding westerly winds aloft that would augment the existing westerly flow, in which case the winds aloft would increase following LBA. However, Figure 3 clearly shows that for the composite lake breeze presented here the westerly flow actually decreases in magnitude following LBA. An examination of the individual u wind components for each of the cases shows that the 12 June case may exhibit return flow above 1.25 km; the other cases do not have lidar observations at that height due to a lack of sufficient aerosol scattering on those days. Lyons (1972) showed return flow for Chicago-area lake breezes tended to peak around 1500 m AGL. Therefore, the return flow in these cases may simply be beyond the range of the lidar.

b. Baroclinicity and Circulation

Time/height cross sections of pressure and density can be seen in Figure 4. Since there are not corresponding high-temporal resolution profiles over the lake, a definitive characterization of the baroclinicity of the environment cannot be made. However, the rate at which density changes relative to pressure can inform as to how quickly the environment is becoming more or less baroclinic. At the start of the analysis period, the isopycnals are parallel to isobars at all observed levels at Sheboygan, but daytime heating causes the density to change more quickly than the pressure. At Zion, the isobars and isopycnals are already intersecting at the start of the analysis, but the later LBA time means more heating has taken place. Below 300 meters at Sheboygan (and throughout the entire depth of observations at Zion), the isopycnals slope downward in the time/height cross section meaning that the atmosphere is becoming less dense with time as it approaches LBA. At the same time, close inspection of Figure 4 shows a slight upward slope in the isobars compared to the horizontal lines of the altitude grid. Once the lake breeze arrives, the

slope of the isopycnals with respect to time reverses sign as the atmosphere rapidly becomes more dense with the arrival of the cold, dry air. After approximately one hour, the isopycnals and isobars are parallel again, which is consistent with a barotropic atmosphere. The density of the lake breeze-advected air is greater at Sheboygan than it is at Zion, behavior that is expected given the disparity in temperatures between the two locations. When combined, the profiling observations at Sheboygan and Zion are consistent with the solenoidal characterization of lake breeze circulations described earlier. It is important to note that the TROPoe retrieval algorithm derives the thermodynamic variables on a height grid and then calculates the pressure hypsometrically which assumes that the atmosphere is in hydrostatic balance. While the small horizontal scale of sea breezes means that they do not necessarily behave hydrostatically, numerical modeling studies (e.g. Yang 1991) indicate that there is little difference between hydrostatic and nonhydrostatic simulations of weak sea breezes. Therefore, any error in the isobars in Figure 4 due to a lack of hydrostatic balance is likely to be small.

The role of pressure and density in generating a lake breeze can be further explored by using Equation 1 to calculate how the thermodynamic state at a given time forces changes in the circulation with time. Results using the composite AERI profiles at Sheboygan integrated over several different depths of the atmosphere are shown in Figure 5. Regardless of the integration depth, the rate of change of circulation before LBA is close to zero or slightly negative. However, there is a substantial increase in the circulation rate at 0 h LBA, coincident with the observed shift in surface winds. This increase is visible at all analyzed heights, though the value for the 20 m layer is less than half of the values for the deeper layers. The values for 100 m and 200 m depth are neutral to positive for 1.5 h after LBA, which indicates that the lake breeze circulation continues to intensify after the time of LBA, coincident with the continued turning of the winds as

observed by the DLID during that period. Altogether, these data are consistent with the theory that the lake breeze is actually a change in circulation that arises from local density differences. The observations at Zion (not shown) did not indicate similar behavior, although this is more likely an artifact of the coarse vertical resolution of the MWR rather than a product of any atmospheric difference at Zion.

c. Inland Penetration and Low Level Structure

One of the ways in which individual lake breeze events differ is the degree to which they penetrate inland. Certain lake breezes remain near-shore, impacting the conditions only within a few hundred meters of the shore or less, while others can extend hundreds of kilometers inland (Sills et al. 2011). To investigate the role of vertical structure on inland penetration, the events were classified into "near-shore" or "inland" based on observed winds at inland sites. These inland observations came from two air quality monitoring sites operated by the Wisconsin Department of Natural Resources: Kenosha Water Tower, 5.7 km inland from the shore and 15 km northwest of Zion; and Sheboygan Haven, 5.3 km inland from the shore and 10 km northwest of Sheboygan. The locations of these sites relative to the Zion and Sheboygan supersites are marked on Figure 1. If an observed wind at the inland site experienced a shift in wind direction that was consistent with the lake breeze for 3 h or more, it was considered to represent an inland lake breeze event. Based on these criteria, three of the six events at Zion were classified as inland events while all but one event at Sheboygan were classified as such; these events are identified in Table 2 in bold type. To assess what, if any, role instability may have had in the penetration distance of the lake breezes, data from the AERI and MWR profilers were used to calculate the vertical rate of change of equivalent potential temperature θ_e. Results are displayed in Figure 6. Positive (negative) values

for $d\theta_e/dz$, representing convectively stable (unstable) conditions, are shaded in red (blue). While the small sample size makes it difficult to draw definitive conclusions, at least for the events observed here, the inland lake breeze cases tended to form in more unstable environments (as evidenced by the blue shading above the near-surface layer) than the near-shore cases (which have more pink shading in the lowest 500 m). This is an interesting finding that stands in contrast to theory (Rotunno 1983, Walsh 1974), which states that the length scale of inland penetration of sea breezes is proportional to stability. However, modeling studies (e.g. Xian and Pielke 1991) have found that more unstable environments produce lake breezes with deeper penetrations. The Doppler lidar observations at Sheboygan indicate some correspondence between the strength of the pre-existing westerly flow and whether a lake breeze penetrates inland or not, as the pre-LBA winds aloft in the sole near-shore case (12 June 2017) are stronger than the mean winds aloft of the inland cases. This is consistent with findings by Curry et al. (2017) and Mariani et al. (2018), who note that stronger offshore winds hinder the inland progression of the lake breeze front. It may be that the preexisting flow, not the local convective stability, is the most important parameter for determining the degree of penetration. Doppler lidar observations at Sheboygan for the single near-shore case were absent for most of the post-LBA period. As a result, this study is unable to fully address the relative importance of stability versus wind speed in determining the degree of inland penetration.

The Zion sodar has a fine vertical resolution (10 m) and narrow dead band at the surface (30 m), and so it is well-suited for investigating the structure of the lake breeze in greater detail. Figure 7 shows the time-height cross section of the mean zonal (u) and vertical (w) components of the sodar-observed winds during both the inland and near-shore cases; recall that there is an identical number (3) of events of each type at Zion. Since the shoreline at Zion is oriented in a due

north-south direction, the u component of the wind effectively represents the cross-shore flow and a switch in the sign from positive to negative represents passage of the lake breeze front. It is clear from the results that, regardless of breeze type, the lake breeze front is a near-vertical wall approximately 100 m deep that arrives right at LBA and disrupts the predominately westerly flow. In the hours that follow, the near-shore cases exhibit little deepening from that initial impulse as the negative values for u remain limited to the lowest 100 m of the troposphere. The inland cases, however, quickly show growth in the depth of the system to at least double their initial height. As noted above, the inland cases formed in more unstable environments. However, the contemporaneous vertical velocity observations indicate that thermodynamic instability is not likely to be the reason for the discrepancy in the two breeze types as the magnitudes of the vertical motion are largely similar during and following LBA for both breeze types. The strongest vertical lifting is found right at LBA as the arriving cold air acts as a density current and displaces the shoreline air upward. Following LBA, there is a hint of periodicity in the upward motion, especially in the near-shore (stable) cases where positive vertical velocities are seen starting 30 min after LBA with a frequency of approximately 1 h. It is unlikely that these structures are thermals embedded in the convective boundary layer [as documented by Curry et al. (2017)] as these are occurring on a longer time scale and are the result of multiple cases being averaged together. Rather, they may represent a standing wave formed when the westerly pre-existing flow collides with the dense air of the lake breeze. In this case, one would expect vertical velocity couplets in both near-shore and inland cases, but the pattern would be more pronounced in the near-shore cases due to their association with stronger westerly flow. The inland (unstable) cases tend towards more pronounced periods of vertical lift following LBA. However, these times are not well-correlated with the vertical growth of the onshore flow. In fact, the lake breeze

519 experiences its greatest vertical extent at the same time that the atmosphere is undergoing its most
520 consistent period of subsidence. This tends to rule out momentum advection due to thermodynamic
521 instability as a cause for growth of the lake breeze layer. Since the MWR observations indicate
522 that the cold pool is not deepening with time, a more likely solution is that an onshore perturbation
523 horizontal pressure gradient force has developed aloft, producing a sloped interface along the
524 advancing lake breeze front.
525
526 **5. Aerosol Impacts**
527 The HSRL deployed at Sheboygan allows for the observation of absolutely-calibrated
528 profiles of aerosol backscatter. Molecular backscattering often obscures the contributions of
529 aerosols in traditional backscatter lidars, but the HSRL technique is able to separate and remove
530 molecular scattering from the observed backscatter. During two of the six lake breezes observed
531 at Sheboygan, enhanced aerosol backscatter was observed by the HSRL at the same altitude and
532 time as the Doppler lidar observed the wind shift. These two cases can be seen in Figure 8, which
533 shows the time/height cross section of the base-10 logarithm of the aerosol backscatter cross
534 section. In both cases (and in other cases not presented here) the growth of the boundary layer with
535 solar heating can be seen as the increasing depth over which enhanced backscatter is visible
536 starting before LBA but continuing after; this is especially apparent in the 2 June case in which
537 the growth is easily visible starting nearly 3 h before LBA. After the growth in the depth of the
538 lake breeze is significant enough that it can be observed by the Doppler lidar, both cases show
539 additional enhanced backscatter coincident with the shifting wind barbs, though it is more subtle
540 on 2 June than 16 June. This is consistent with the lake breeze containing, on average, a slight
541 enhancement in fine aerosols.

Increases in fine and ultrafine aerosol number concentrations were also observed around the time of LBA at Zion. Figure 9a shows the aerosol size distribution while Figure 9b shows the times series of particulate matter with aerodynamic diameter less than 2.5 micron ($PM_{2.5}$). In the composite average, aerosols at sizes of 20-80 nm increase dramatically at the time of LBA. Similar graphs made for non-lake breeze days (not shown) do not show the 20-80 nm enhancement. The mean quantitative increase in the total aerosol number is from 8413 cm^{-3} (pre LBA) to 12,435 cm^{-3} (post LBA), and was statistically significant using a two-sample t-test. At the size where the post-LBA feature is most notable (38 nm), the size distribution function increases in height by a factor of 2.7.

Changes in other aerosol variables at Zion were investigated as well, including aerosol optical depth, integrated aerosol volume, and $PM_{2.5}$. As shown in Figure 9b, for the 3 h period before LBA to the 3 h period after LBA, $PM_{2.5}$ increased by 2.5 μg m^{-3} on lake breeze days. This increase was greater than the increase on non-lake breeze days (0.6 μg m^{-3}); for non-lake breeze days, the average LBA time at Zion was used as the time to determine the relative difference. This difference was found to be statistically significant using a two-sample t-test ($p=0.02$). In situ integrated aerosol volume increased as well, consistent with the increases in aerosol number and $PM_{2.5}$. The increases in aerosol volume and $PM_{2.5}$ were not as distinct at the time of LBA as the change in ultrafine aerosol number, but rather suggested increasing mass of secondary aerosol in the air coming off the lake at later times in the day.

AOD at 550 nm on lake breeze days (not shown) ranged from approximately 0.03 to 0.22, and AOD at 331 nm ranged from approximately 0.08 to 0.43. However, the AOD data were too sparse to create a composite time series or inspect for discontinuities at the LBA time. In a study in Toronto, increases in AOD and surface and vertical column density NO_2 were observed at LBA

565 time (Davis et al. 2020), but direct comparisons cannot be drawn due to differences in land use,
566 nearby sources, and fetch of the observation sites.

567 The general conceptual model of lake breeze pollution episodes in the region (Dye et al.
568 1995), supported by LMOS 2017 results in Hughes et al. (2021) and Doak et al. (2021), suggest
569 that much of the aerosol signal seen after LBA is due to anthropogenic pollution from land-based
570 sources within the Lake Michigan airshed. Oxidation of precursor species leads to secondary
571 aerosol formation in these plumes that are transported over the lake and then returned in the lake
572 breeze. The conceptual model explains the gradual increase in aerosol volume and $PM_{2.5}$ seen after
573 LBA, and the greater increase (afternoon vs. morning) on lake breeze days vs. non-lake breeze
574 days. However, the conceptual model does not explain the distinct increase in ultrafine aerosol
575 seen at the LBA time. This is consistent with ultrafine aerosols generating from breaking of
576 freshwater waves (Slade et al. 2010, Axson et al. 2016); however, combustion sources over the
577 lake, gas-to-particle nucleation over the lake (likely in land-based anthropogenic plumes), and
578 other potential sources are possible. Other observations such as time-resolved measurements of
579 wave state, ultrafine aerosol chemistry, and vertical profiles of aerosols would be required to
580 elucidate specific contributions.

581

582

583

584 **6. Synthesis and Conclusions**

585 As part of the 2017 Lake Michigan Ozone Study, ground-based supersites were deployed
586 at two locations adjacent to the western shore of Lake Michigan. The unique combination of
587 kinematic and thermodynamic profilers at each site enables the analysis of lake breeze structure in

588 unprecedented detail, and a compelling portrait of the development of this phenomenon emerges
589 from the synthesis of these instruments and surface measurements.

590 These observations show that lake breezes during LMOS 2017 developed as follows. In
591 the absence of synoptic forcing, a preexisting inversion can be found over the land in the overnight
592 hours with predominately westerly flow throughout the lower troposphere. Background aerosol
593 concentrations show little difference from average values during this time of the year. Following
594 sunrise, several significant changes begin to take place in the lower troposphere. Over the next
595 three to four hours solar heating increases the surface temperature and the depth of the PBL while
596 increased mixing erodes the previous inversion; analysis of the potential temperature profiles (not
597 shown) indicates that the lower PBL becomes largely isentropic with height during this time.
598 While the air over land warms, the temperature of the air over the lake remains largely unchanged.
599 As a result, the density of the air over land becomes much less than over water, which results in
600 sloping isopycnals as observed by the thermodynamic profilers and an increase in baroclinicity.
601 Since the change in the circulation around a fluid element is a function of the magnitude of the
602 baroclinicity, a circulation in the vertical plane develops that is superimposed over the pre-existing
603 westerly flow. Up to this point, there is little change in the winds as the preexisting circulation in
604 the vertical plane is small. However, the baroclinic forcing results in a sudden increase in the
605 circulation which manifests itself as the lake breeze. The change in circulation derived from
606 baroclinicity is well-captured by the ground-based profilers.

607 The lake breeze front is on the order of 100 - 200 m deep and represents the leading edge
608 of the air that has been cooled by conduction of heat into Lake Michigan. This air mass is advected
609 over the land by the lower branch of the lake breeze circulation, and as it advances it forces an
610 updraft that the wind profilers indicate is on the order of 1-2 m s^{-1}. The concentration of aerosols

611 having a diameter of 20 – 80 nm increases to nearly an order of magnitude above background
612 levels with passage of the lake breeze front. While the change in $PM_{2.5}$ concentration is not as
613 dramatic, it still shows a marked increase after the lake breeze front. The low level relative
614 humidity over land increases with the passage of the lake breeze front, even as the absolute
615 humidity is steady or even decreasing, owing to the significant decrease in temperature. Changes
616 in the local thermodynamics result in decreased baroclinicity in the lower troposphere, and the
617 lake breeze circulation achieves a steady state within a few minutes with little change in wind
618 speed or direction observed in the lowest 100 m after that time.

619 The local near-surface environment has been generally stabilized by the lake breeze as
620 evidenced by strong increases in potential temperature with height in the lowest 100 - 200 m. The
621 advancing cold air undercuts the warm air over land and lifts it, creating a strong inversion on the
622 order of 8 K over just 200 m. While the aforementioned lifting can force cloud development along
623 the lake breeze front, the strong stabilization of the atmosphere behind the front results in clearing
624 skies, as seen in the satellite imagery in Figure 1.

625 Some questions remain about the reasons behind the different characteristics observed at
626 the two sites. For example, the difference between the air and lake temperatures is nearly identical
627 between the two sites in the period leading up to LBA, but there is substantial divergence in the
628 temperature differences following LBA as the ensuing gradient is twice as strong at Zion as at
629 Sheboygan. At the same time, the absolute moisture content of the air at Zion seems to be
630 unaffected by the lake breeze while it drops by nearly half at Sheboygan. It is important to
631 remember that there are slight differences in the set of cases used for analysis, as both the coldest
632 day pre-LBA at Sheboygan and the warmest day post-LBA at Zion were the two event days on
633 which there was no corresponding breeze at the other site. This would help bias the respective

sites in opposite directions. The two sites themselves are not situated identically, either, as the Sheboygan site was much closer to the shore than the Zion site (230 m vs. 1 km). The longer fetch at Zion combined with the relatively slow speed at which lake-cooled air is advected over the warmer land means that the air can undergo substantially more modification at that site than Sheboygan. The degree of urban development also provides an interesting contrast between the two sites. At the microscale, the Sheboygan site was more urbanized as it was deployed next to a resort development while the Zion site was within a state park. However, the community of Sheboygan is a discrete smaller city surrounded by farmland while Zion is in the heart of the urban amalgamation that lies between Chicago and Milwaukee. The degree to which these different settings may be impacting the characteristics of the lake breeze is an important question, but one that is beyond the scope of the present work.

This work covers a relatively small number of cases along one shore of just one of the Great Lakes. Additional observations at other locations are needed to determine if the behaviors observed here are also seen at bodies of water with different shoreline geometries, surface area, water depths, climate regimes, and other qualities that can impact water/land/atmosphere interactions. For future observational studies of lake or sea breeze structure, an ideal observing site would contain both a sodar and a Doppler lidar so that a more complete profile of winds over the lowest kilometer of the atmosphere could be observed since the sodar would fill in all but the very lowest level of the lidar's dead band. When coupled with an AERI and in situ surface meteorology sensors, this would provide a near-continuous profile of atmospheric thermodynamics and kinematics from the surface to the maximum effective range of the lidar.

Acknowledgements

The authors are indebted to David Turner, who assisted with applying the TROPoe algorithm to the microwave radiometer data. Steve Smith assisted with deployment of the radiometer and sodar at Zion while Erik Olson led the deployment of SPARC at Sheboygan. David Loveless and Coda Phillips (University of Wisconsin – Madison) and Jack Bruno (Ohio University) monitored the SPARC. Funding for the SPARC trailer deployment and the University of Northern Iowa's participation at Zion during LMOS 2017 was provided by the GOES-R Program Office via the NOAA Cooperative Agreement with the Cooperative Institute for Meteorological Satellite Studies (NA15NES432001). The three anonymous reviewers contributed many insightful comments and suggestions that greatly improved this paper. This work was funded in part by the National Science Foundation under Grant AGS-1712909, AGS-1713001, and AGS-1712828.

Data availability statement

Profiler data used in this study are freely available from the LMOS 2017 campaign archive at https://www-air.larc.nasa.gov/missions/lmos/index.html. Inland wind observations were obtained from the EPA Air Quality System at https://aqs.epa.gov/aqs/.

References

Abdioskouei, M., Z. Adelman, J. Al-saadi, T. Bertram, G. Carmichael, M. Christiansen, P. Cleary, A. Czarnetzki, A. Dickens, M. Fuoco, M. Harkey, L. M. Judd, D. Kenski, D. Millet, R. B. Pierce, C. Stanier, B. Stone, J. Szykman and T. Wagner (2019). 2017 Lake Michigan Ozone Study (LMOS) Preliminary Finding Report. Available at

https://www.ladco.org/wp-content/uploads/Research/LMOS2017/LMOS_LADCO_report_revision_apr2019_final.pdf

Axson, J. L., N. W. May, I. D. Colon-Bernal, K. A. Pratt and A. P. Ault, 2016: Lake spray aerosol: a chemical signature from individual ambient particles. *Environ. Sci. Technol.*, **50**, 9835-9845.

Banta, R. M., L. D. Olivier, and D. H. Levinson, 1993: Evolution of the Monterey Bay sea-breeze layer as observed by a pulsed Doppler lidar. *J. Atmos. Sci*, **50**, 3959 – 3982.

Blumberg, W. G., D. D. Turner, U. Löhnert, and S. Castleberry, 2015: Ground-based temperature and humidity profiling using spectral infrared and microwave observations. Part II: actual retrieval performance in clear-sky and cloud conditions. *J. Appl. Meteor. Climatol.*, **54**, 2305 – 2319.

Clough, S. A., M. W. Shepard, E. J. Mlawer, J. S. Delamere, M. J. Iacono, K. Cady-Pereira, S. Boukabara, and P. D. Brown, 2005: A summary of the AER codes. *J. Quant. Spectrosc. Radiat. Transfer*, **91**, 233-244.

Curry, M., J. Hanesiak, S. Kehler, D. M. L. Sills, and N. M. Taylor, 2017: Ground-based observations of the thermodynamic and kinematic properties of lake-breeze fronts in southern Manitoba, Canada. *Bound.-Lay. Meteor.*, **163**, 143 – 159.

Davis, Z. Y. W., D. M. L. Sills and R. McLaren, 2020: Enhanced NO2 and aerosol extinction observed in the tropospheric column behind lake-breeze fronts using MAX-DOAS. *Atmos. Environ.*, **5**, 100066.

Doak, A. G. and coauthors, 2021: Characterization of ground-based atmospheric pollution and meteorology sampling stations during the Lake Michigan Ozone Study 2017. *J. Air Waste Manag. Assoc.*, **71**, 866 – 889.

Dye, T. S., P. T. Roberts, and M. E. Korc, 1995: Observations of transport processes for ozone and ozone precursors during the 1991 Lake Michigan Ozone Study. *J. Appl. Meteor.*, **34**, 1877 – 1889.

Ebell, K., E. Orlandi, A. Hünerbein, U. Löhnert, and S. Crewell, 2013: Combining ground-based with satellite-based measurements in the atmospheric state retrieval: Assessment of the information content. *J.Geophys. Res. Atmos.*, **118**, 6940 – 6956.

Eloranta, E.W., 2005: High spectral resolution lidar. *Lidar: Range-Resolved Optical Remote Sensing of the Atmosphere*, K. Weitkamp, Ed. New York: Springer-Verlag, pp. 143–163.

Finkele, K., J . M. Hacker, H. Kraus, and R. A. D. Byron-Scott, 1995: A complete sea-breeze circulation cell derived from aircraft observations. *Bound.-Layer. Meteor.*, **17**, 299 – 317.

Herman, J., A. Cede, E. Spinei, G. Mount, M. Tzortziou, and N. Abuhassan, 2009: NO_2 column amounts from ground-based Pandora and MFDOAS secrometers using the direct-sun DOAS technique: Intercomparisons and application to OMI validation. *J. Geophys. Res.-Atmos.*, **114**, doi: 10.1029/2009JD011848.

Holben, B. N. and coauthors, 1998. AERONET—A federated instrument network and data archive for aerosol characterization. *Remote Sens. Environ.*, **66**, 1-16.

Holton, J., 1992: *An Introduction to Dynamic Meteorology*, third ed., San Diego: Academic Press, 511 pp.

Hughes, D. D., and coauthors, 2021: $PM_{2.5}$ chemistry, organosulfates, and secondary organic aerosol during the 2017 Lake Michigan Ozone Study. *Atmos. Environ.*, **244**, 117939.

724 Keen, C. S. and W. A. Lyons, 1978: Lake/land breeze circulations on the western shore of Lake
725 Michigan. *J. Appl. Meteor.*, **17**, 1843 – 1855.
726 King, P. W. S., M. J. Leduc, D. M. L. Sills, N. R. Donaldson, D. R. Hudak, P. Joe, and P. B.
727 Murphy, 2003: Lake breezes in southern Ontario and their relation to tornado climatology.
728 *Wea. Forecasting*, **18**, 795 – 807.
729 Knuteson, R. O. and coauthors, 2004a: Atmospheric Emitted Radiance Interferometer. Part I:
730 Instrument design. *J. Atmos. Oceanic Technol.*, **21**, 1763 – 1776.
731 Knuteson, R. O. and coauthors, 2004b: Atmospheric Emitted Radiance Interferometer. Part II:
732 Instrument performance. *J. Atmos. Oceanic Technol.*, **21**, 1777 – 1789.
733 Laird, N., D. R. Kristovich, X.-Z. Liang, R. W. Arritt, and K. Labas, 2001: Lake Michigan lake
734 breezes: Climatology, local forcing, and synoptic environment. *J. Appl. Meteor.*, **40**, 409
735 – 424.
736 Levy, I., P. A. Makar, D. Sills, J. Zhang, K. L. Hayden, C. Mihele, J. Narayan, M. D. Moran, S.
737 Sjostedt, and J. Brook, 2010: Unravelling the complex local-scale flows influencing ozone
738 patterns in the southern Great Lakes of North America. *Atmos. Chem. Phys.*, **10**, 10895 –
739 10915.
740 Loveless, D. M., T. J. Wagner, D. D. Turner, S. A. Ackerman, and W. F. Feltz, 2019: A composite
741 perspective on bore passages during the PECAN campaign. *Mon. Wea. Rev.*, **147**, 1395 –
742 1413.
743 Lyons, W. A., 1970: Numerical simulation of Great Lakes summertime conduction inversions.
744 *Proc. 13th Conf. Great Lakes Res*., Intl. Assoc. Great Lakes Res., 369-387.
745 Lyons, W. A., 1972: The climatology and prediction of the Chicago lake breeze. *J Appl, Meteor.*,
746 1259 – 1270.

747 Lyons, W. A and H. S. Cole, 1976: Photochemical oxidant transport: mesoscale lake breeze and
748 synoptic-scale aspects. *J. Appl. Meteor.*, **15**, 733 – 743.
749 Mariani, Z., A. Dehghan, P. Joe and D. Sills, 2018: Observations of lake-breeze events during the
750 Toronto 2015 Pan-American Games. *Bound.-Layer Meteor.*, **166**, 113 -135.
751 Martin, J. E., 2006: *Mid-Latitude Atmospheric Dynamics: A First Course*., West Sussex: John
752 Wiley & Sons, 324 pp.
753 Mastrantonio, G., A. P. Viola, S. Argentini, G. Fiocco, L. Giannini, L. Rossini, G. Abbate, R.
754 Ocone, and M. Casonato, 1994: Observations of sea breeze events in Rome and the
755 surrounding area by a network of Doppler sodars. *Bound.-Lay. Meteor.*, **71**, 67 – 80.
756 Miller, S. T. K., B. D. Keim, R. W. Talbot, and H. Mao, 2003: Sea breeze: Structure, forecasting,
757 and impacts. *Rev. Geophys.*, **43**, doi: 10.1029/2003RG000124.
758 Pearson, G., F. Davies, and C. Collier, 2009: An analysis of the performance of the UFAM pulsed
759 Doppler lidar for observing the boundary layer. *J. Atmos. Oceanic Technol.*, **26**, 240 –
760 250.
761 Prakash, J. W. J., R. Ramachandran, K. N. Nair, K. S. Gupta, and P. K. Kunhikrishnan, 1992: On
762 the structure of sea-breeze fronts observed near the coastline of Thumba, India. *Bound.-*
763 *Lay. Meteor.*, **59**, 111-124.
764 Rotunno, R. On the linear theory of the land and sea breeze. *J. Atmos. Sci.*, **40**, 1999 – 2009.
765 Schwab, D. J., G. A. Keshkevich, and G. C. Muhr, 1999: Automated mapping of surface water
766 temperature in the Great Lakes. *J. Great Lakes Res.*, **25**, 468 – 481.
767 Scott, R. W. and F. A. Huff, 1996: Impacts of the Great Lakes on regional climate conditions. *J.*
768 *Great Lakes Res.*, **22**, 845 – 863.

769 Segal, M., M. Leuthold, R. W. Arritt, C. Andersen, and J. Shen, 1997: Small lake daytime breezes:
770 Some observational and conceptual evaluations. *Bull. Amer. Meteor. Soc.*, **78**, 1135 – 1147.
771 Shen, S., P. A. Jacques, Y. Zhu, M. D. Geller, and C. Sioutas, 2002: Evaluation of the SMPS-APS
772 system as a continuous monitor for measuring $PM_{2.5}$, PM_{10}, and coarse ($PM_{2.5-10}$)
773 concentrations. *Atmos. Environ.*, **36**, 3939 – 3950.
774 Shipley, S. T., D. H. Tracy, E. W. Eloranta, J. T. Trauger, J. T. Sroga, F. L. Roesler, and J. A.
775 Weinman, 1983: A High Spectral Resolution Lidar to measure optical scattering properties
776 of atmospheric aerosols. Part I: Instrumentation and theory. *Appl. Optics*, **23**, 3716 – 3724.
777 Sills, D. M., J. R. Brook, I Levy, P. A. Makaer, J. Zhang, and P. A. Taylor, 2011: Lake breezes in
778 the southern Great Lakes region and their influence during BAQS-Met 2007. *Atmos.*
779 *Chem. Phys.*, **11**, 7955 – 7973.
780 Simpson, J. E., 1994: *Sea breeze and local wind.* New York: Cambridge University Press. 244
781 pp.
782 Slade, J. H., T. M. VanReken, G. R. Mwaniki, S. Bertman, B. Stirm and P. B. Shepson, 2010:
783 Aerosol production from the surface of the Great Lakes. *Geophys. Res. Let.*, **37**, L18807.
784 Smirnov, A., B. N. Holben, T. F. Eck, O. Dubovik, and I. Slutsker, 2000. Cloud-screening and
785 quality control algorithms for the AERONET database. *Remote Sens. Environ.*, **73**, 337-
786 349.
787 Stanier, C. O. and coauthors, 2021: Overview of the Lake Michigan Ozone Study 2017. *Bull.*
788 *Amer. Meteor. Soc.*, available in early online release.
789 Turner, D.D., R. O. Knuteson, H. E. Revercomb, C. Lo, and R. G. Dedecker, 2006: Noise
790 reduction of Atmospheric Emitted Radiance Interferometer (AERI) observations using
791 principal component analysis. *J. Atmos. Oceanic Technol.*, **23**, 1223 – 1238.

792 Turner, D. D. and U. Löhnert, 2014: Information content and uncertainties in thermodynamic
793 profiles and liquid cloud properties retrieved from the ground-based Atmospheric Emitted
794 Radiance Interferometer (AERI). *J. Appl. Meteor. Climatol.*, **53**, 752 -771
795 Turner, D. D. and U. Löhnert, 2021: Ground-based temperature and humidity profiling:
796 Combining active and passive remote sensors. *Atmos. Meas. Tech.* Accepted for
797 publication.
798 Turner, D. D. and W. G. Blumberg, 2019: Improvements to the AERIoe thermodynamic profile
799 retrieval algorithm. *IEEE J. Sel. Topics. Appl. Earth Observ. Remote Sens.* In press.
800 Vermeuel, M. P. and coauthors, 2019: Sensitivity of ozone production to NOx and VOC along
801 the Lake Michigan coastline. *J. Geophys. Res Atmospheres*, **124**, doi:10.1029/
802 2019JD030842
803 Wagner, T. J., D. D. Turner, and P. M. Klein, 2019: A new generation of ground-based mobile
804 platforms for active and passive profiling of the atmospheric boundary layer. *Bull. Amer.*
805 *Meteor. Soc.*, **100**, 137 – 153.
806 Wagner. T. J., W. F. Feltz, and S. A. Ackerman, 2008: The temporal evolution of convective
807 indices in storm-producing environments. *Wea. Forecasting*, **23**, 786 – 794.
808 Xian, Z. and R. A. Pielke, 1991: The effects of width of land masses on the development of sea
809 breezes. *J. Appl. Meteor.*, **30**, 1280 – 1304.
810 Yang, X., 1991: A study of nonhydrostatic effects in idealized sea breeze systems. *Boundary-*
811 *Layer Meteor.*, **54**, 183 – 208.
812
813
814

815

816 **Tables**

817 Table 1: Summary of the instrumentation deployed at the two ground sites used in this study. All
818 data used in this study are publicly available at https://www-air.larc.nasa.gov/missions/lmos/
819

Instrument	**Deployment Site**	**Observation type**	**Approximate Vertical range**	**Temporal resolution**	**Uncertainty**
AERI	Sheboygan	Profiles of temperature, water vapor	0 – 3000 m	2 min	0.9 K, 1.0 g kg^{-1}
Doppler lidar	Sheboygan	Wind vector profiles	140 – 1200 m	1.75 min	0.4 m s^{-1}
HSRL	Sheboygan	Aerosol backscatter profiles	55 – 14600 m	0.5 min	5% of observed value
Microwave radiometer	Zion	Profiles of temperature, water vapor	0 – 3000 m	3 min	1.6 K, 1.4 g kg^{-1}
Sodar	Zion	Wind vector profiles	30 – 200 m	2 min	0.5 m s^{-1}, 2°
Met One AIO	Zion	Temperature, humidity, wind	10 m	1 min	0.2 K, 3% RH, 0.5 , m s^{-1}

SMPS-APS	Zion	Aerosol size distributions	5 m	20 s – 135 s	20% of aerosol diameter
Vaisala WXT 530	Sheboygan	Temperature, humidity, wind	10 m	1 min	0.3 K, 3% RH, 3% wind speed.
AERONET	Zion	Aerosol Optical Depth	Total Column	Variable	±0.1

820

821

Table 2

Dates and times of the identified lake breeze events for the two observation sites during LMOS 2017 as well as lake temperatures from the GLSEA analysis. Times are in UTC; local time is UTC – 5 and local standard time is UTC – 6. Temperatures are in °C. Blanks represent days during which a lake breeze was observed at only one location. Times that have been bolded represent events with inland penetration.

Date	**Time at Sheboygan**	**Time at Zion**	**Sheboygan Lake Temperature (**°C)	**Zion Lake Temperature (**°C)
2 June 2017	**15:42**	**14:48**	9.9	11.8
8 June 2017	**14:49**	**15:16**	10.9	13.1
11 June 2017	**14:32**	17:52	12.1	15.0
12 June 2017	15:43	17:30	12.1	16.1
15 June 2017	--	**17:20**	--	17.4
16 June 2017	**17:41**	17:04	14.5	17.3
17 June 2017	**14:20**	--	14.5	--

Figures

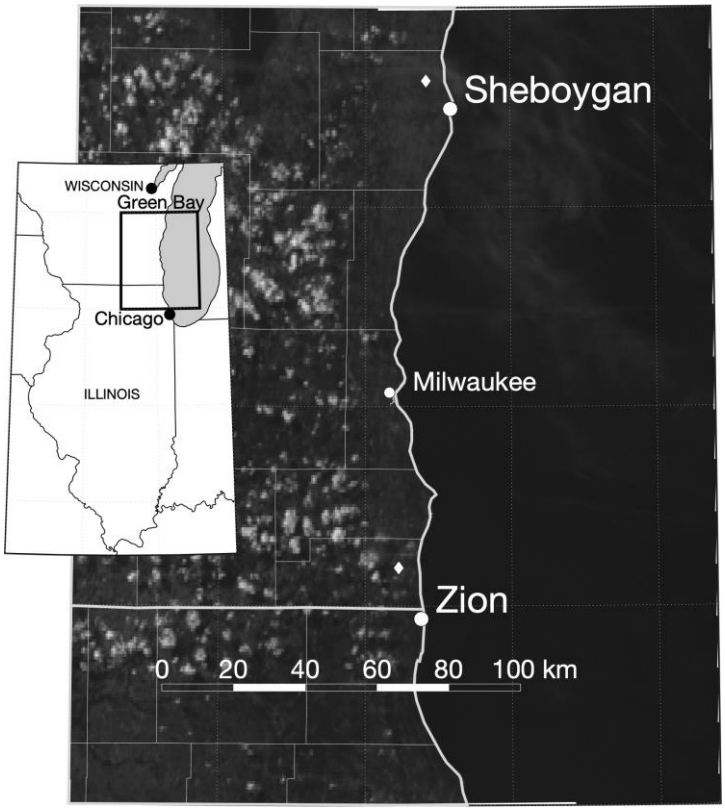

Figure 1. Location of the Sheboygan and Zion supersites along the shore of Lake Michigan, overlaid on GOES-16 0.64 μm reflectance from 2112 UTC on 2 June 2017. Small white diamonds indicate the location of inland monitoring sites used to determine lake breeze penetration. The cities of Chicago, Illinois; and Milwaukee and Green Bay, Wisconsin, are shown for reference. The satellite imagery depicts the lack of convective clouds adjacent to the lake shore frequently seen with mature lake breezes.

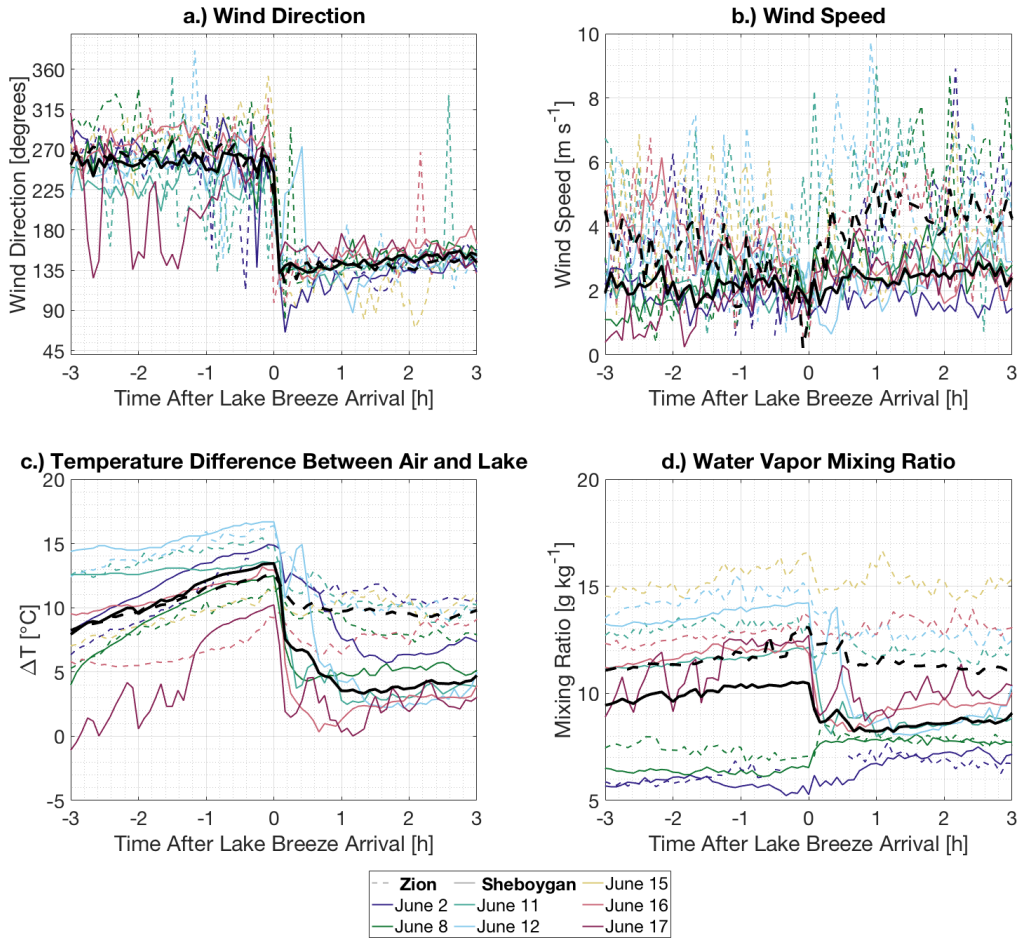

840

841 **Figure 2.** Time series of composited surface conditions for the lake breeze events analyzed in the
842 present study, including a.) wind direction, in degrees; b.) wind speed, in m s^{-1}; c.) the difference
843 between the air temperature and the lake surface temperature as obtained from the GLSEA
844 analysis, in °C; and d.) the water vapor mixing ratio, in g kg^{-1}. Observations from Zion are depicted
845 with a dashed line while observations from Sheboygan are shown with a solid line. The thick black
846 lines represent the mean for each site.

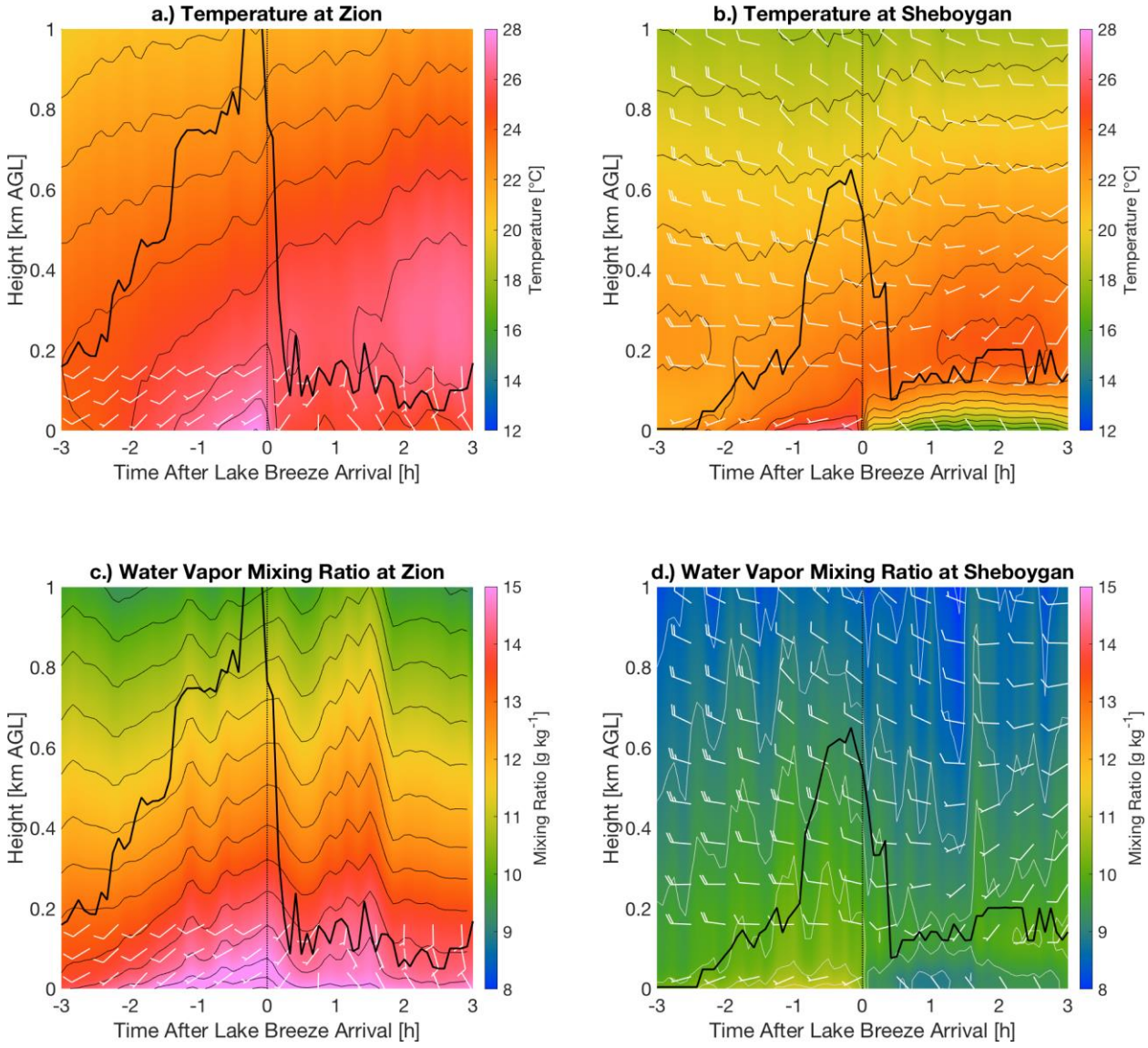

847

848 **Figure 3.** Time-height cross sections of temperature (top row, in °C) and mixing ratio (bottom
849 row, in g kg^{-1}) for the microwave radiometer at Zion (left column) and the AERI at Sheboygan
850 (right column). Winds observed by the sodar at Zion and the Doppler lidar at Sheboygan are
851 overlaid on the respective plots. Winds are shown in kt using the standard convention; this unit
852 was chosen over m s^{-1} so that wind speed magnitudes would be large enough to be displayed with
853 wind barbs. The 10 m surface winds at Sheboygan are appended at the bottom of the plot, but are
854 displaced to the 30 m height for easier viewing. Temperature (mixing ratio) contours are every 1

855 °C (0.5 g kg^{-1}). The thick black line represents the mixing depth calculated from the
856 thermodynamic profiles.
857

858

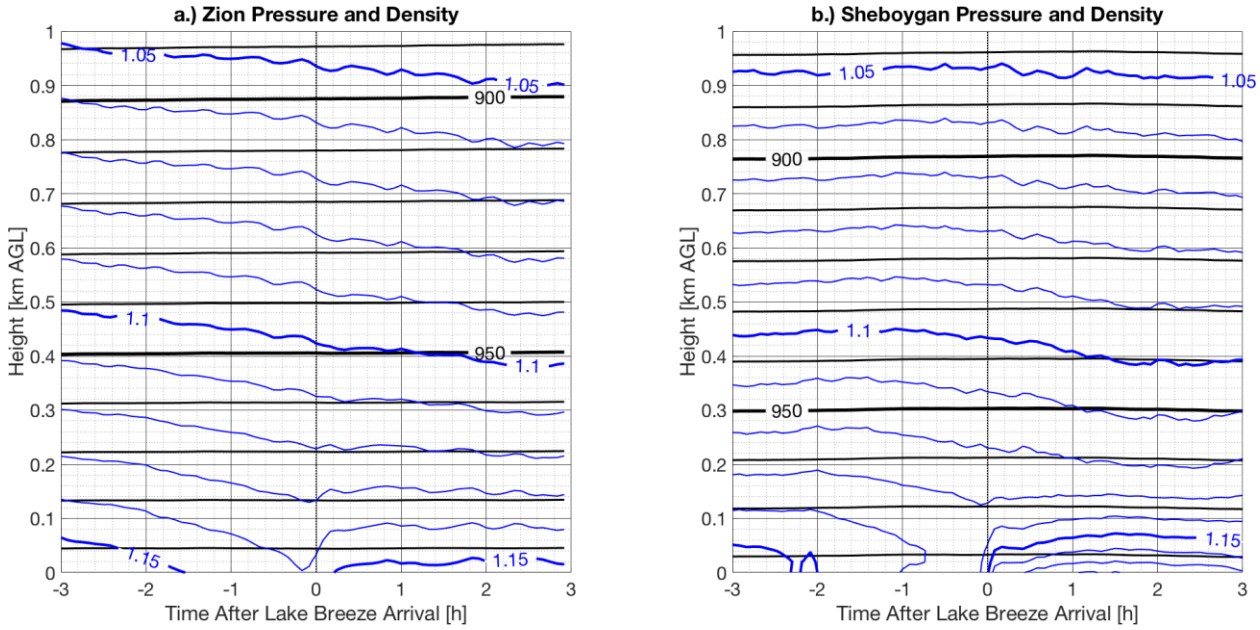

859

860

861 **Figure 4.** Time height cross sections of the mean pressure (black contours, in hPa) and density

862 (blue contours, in kg m^{-3}) for Zion (left) and Sheboygan (right). Pressure contours are drawn

863 every 50 hPa and density contours are drawn every 0.05 kg m^{-3}.

864

865

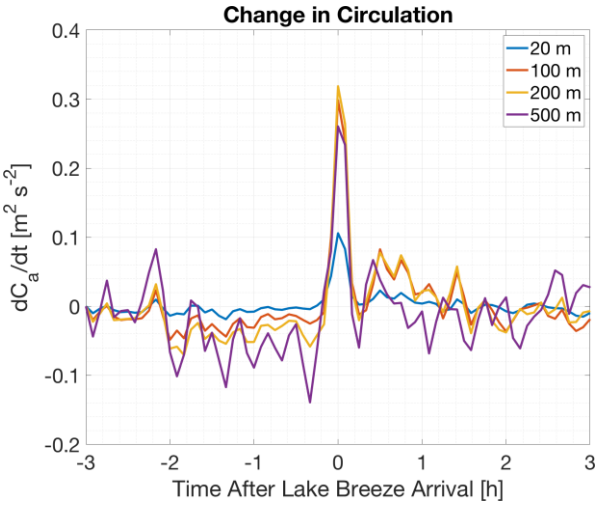

866

867 **Figure 5.** Time series of the temporal rate of change in circulation as derived from AERI

868 thermodynamic profiles. The circulation is evaluated over a layer that extends from the surface

869 to the listed height.

870

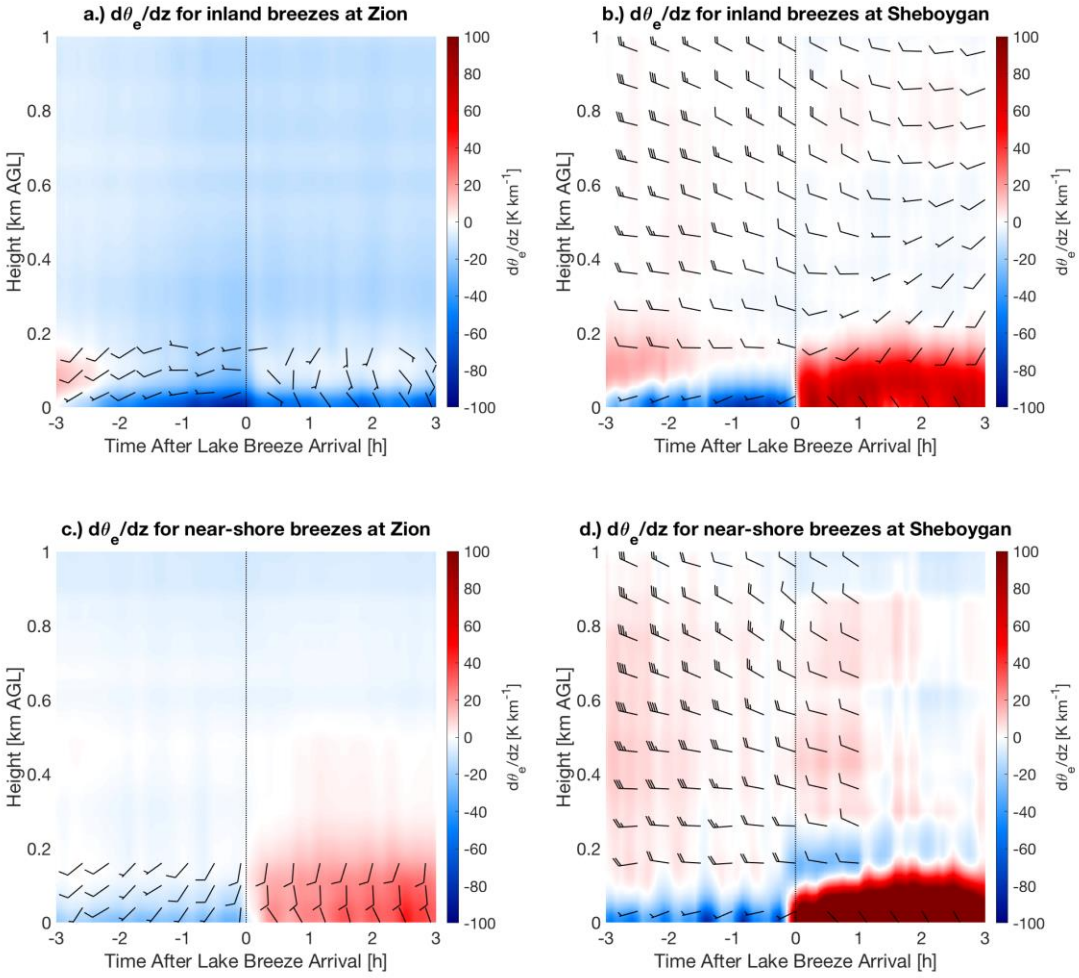

871

872 **Figure 6**. Time/height cross sections of the vertical rate of change of the equivalent potential
873 temperature θ_e for inland breezes (top row) and near-shore breezes (bottom row) at Zion (left
874 column) and Sheboygan (right column). Winds follow the same plotting convention as in Figure
875 3.

876

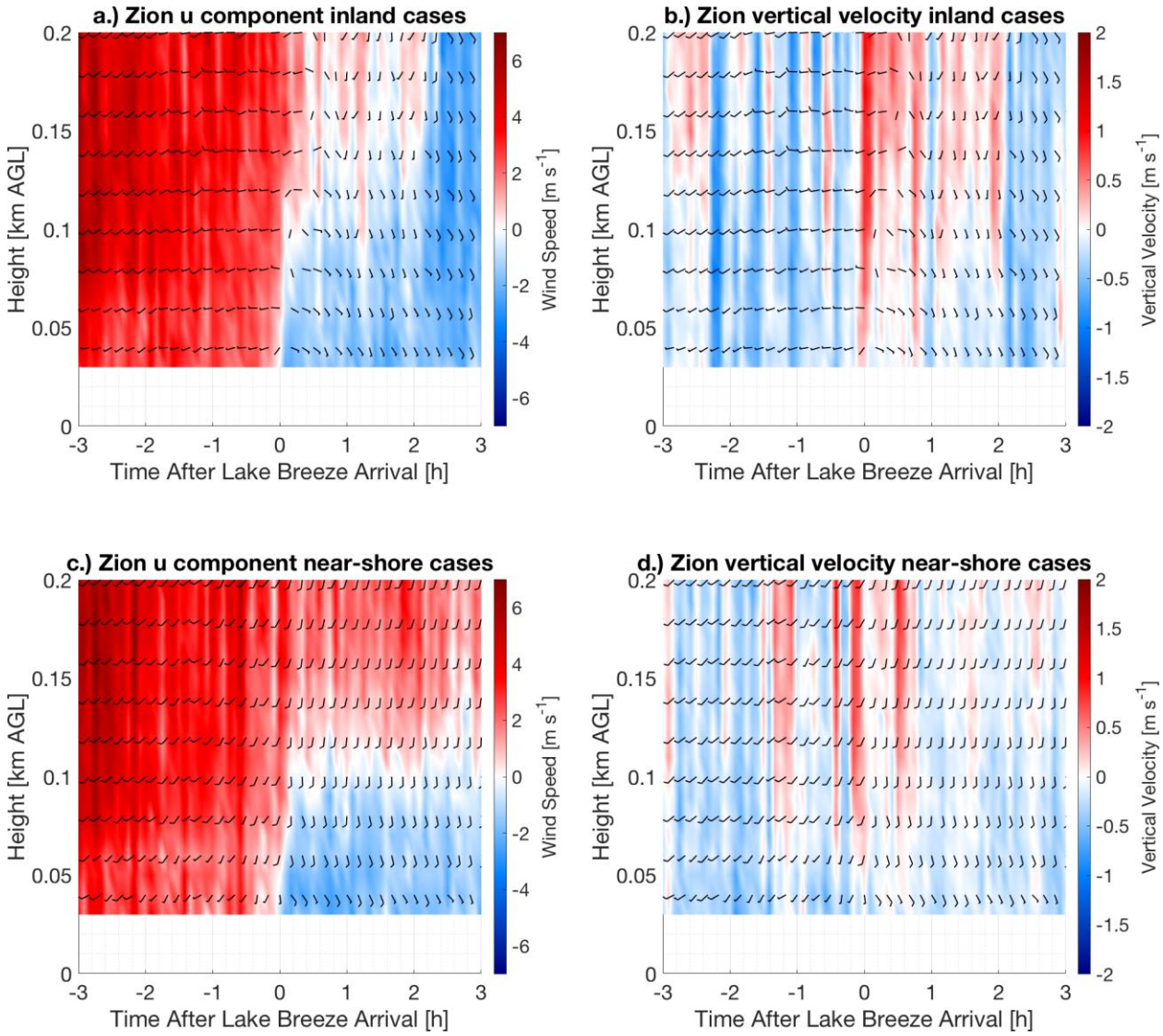

877

878 **Figure 7.** Time/height cross sections of the sodar-observed zonal (u) wind component (left

879 column) and vertical velocity (right column) at Zion for inland (top row) and near-shore (bottom

880 row) lake breezes. Wind barbs are the two dimensional horizontal wind vector, in kts.

881

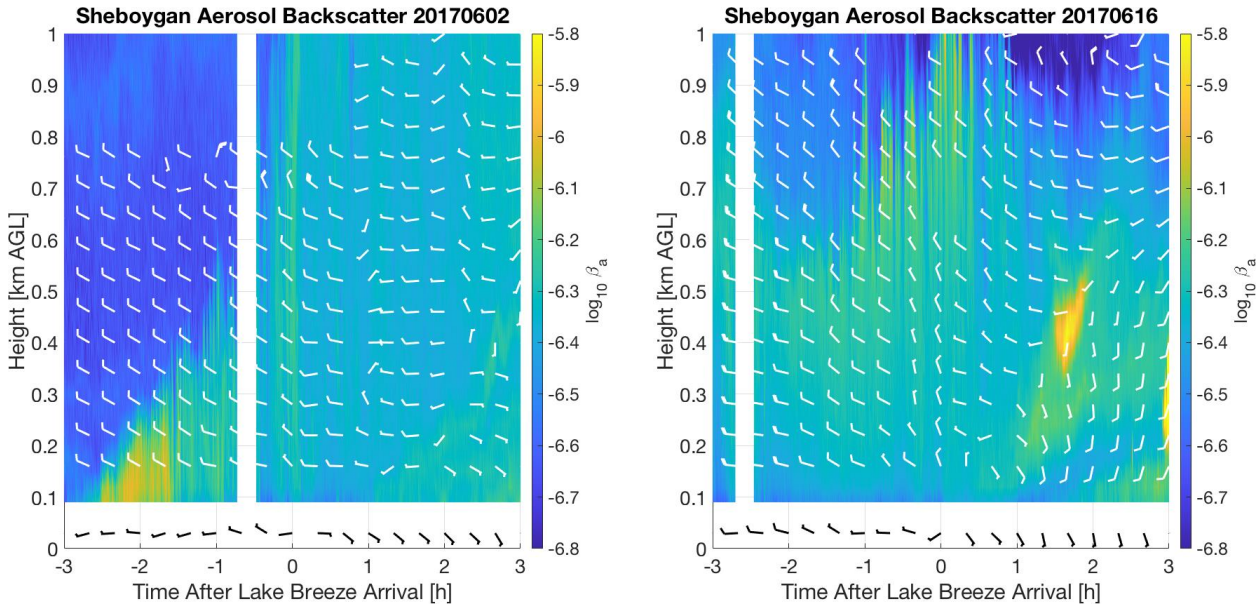

882

883 **Figure 8.** Time/height cross section of aerosol backscatter for two lake breeze cases from the
884 High Spectral Resolution Lidar (HSRL) deployed at Sheboygan. White wind barbs are from the
885 collocated Doppler lidar; black wind barbs are from the 10 m surface wind sensor but are plotted
886 at 30 m to enhance readability. Wind barbs are in kts.

887

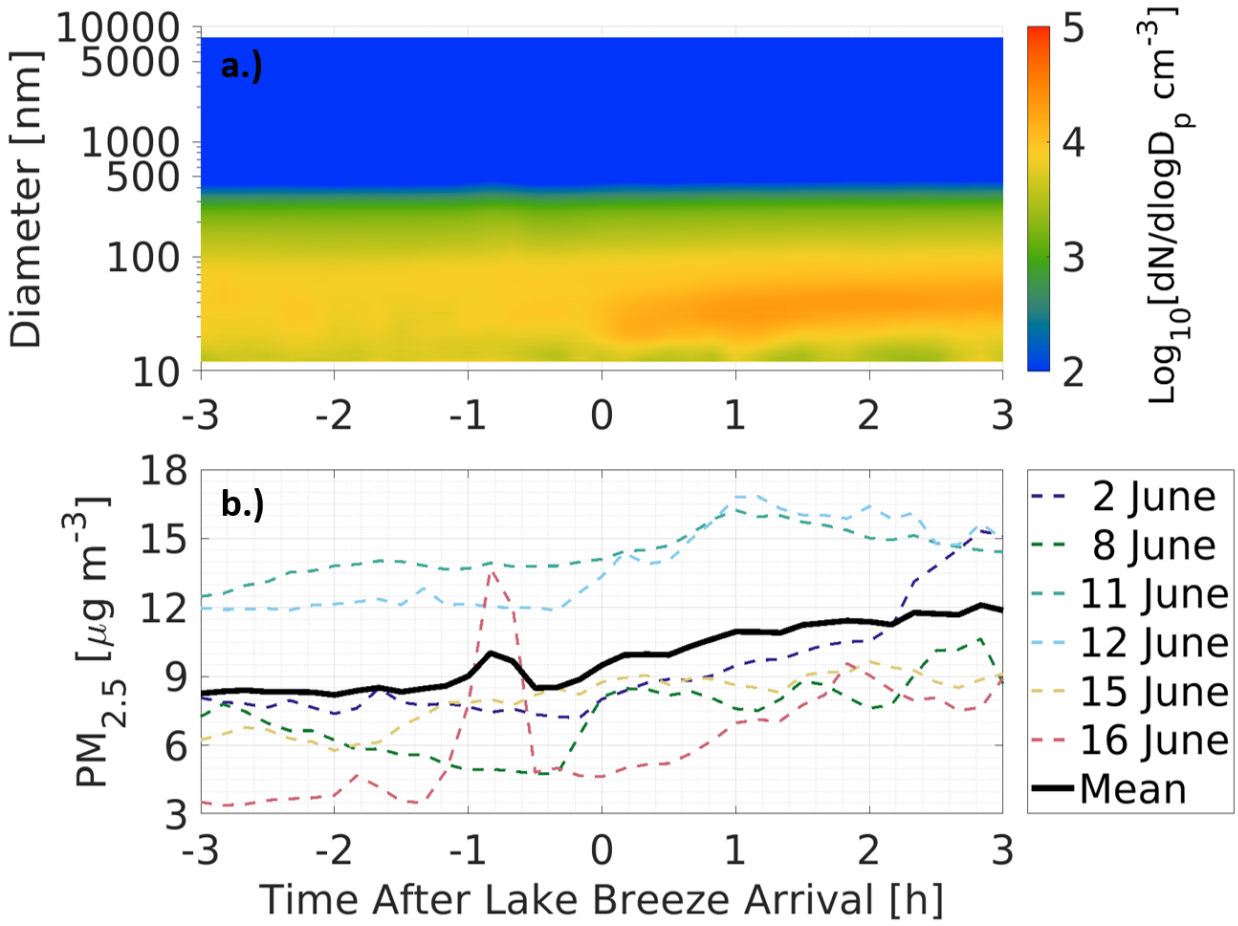

888

889 **Figure 9.** a.) Average aerosol size distribution of all lake breeze days (in base 10 logarithm of

890 cm^{-3}). b.) Time series of calculated $PM_{2.5}$ concentration (in μg m^{-3}) relative to lake breeze arrival

891 time.